GCSF GENE THERAPY FOR PARKINSON'S DISEASE

By

Zachary Lee

A Thesis submitted to the Faculty of

The Charles E. Schmidt College of Medicine

In Partial Fulfillment of the Requirements for the Degree of

Master of Science

Florida Atlantic University

Boca Raton

August 2021

GCSF GENE THERAPY FOR PARKINSON'S DISEASE

by

Zachary Lee

This thesis was prepared under the direction of the candidate's thesis advisor, Dr. Jang Yen Wu, Department of Biomedical Science, and has been approved by all members of the supervisory committee. It was submitted to the faculty of the Charles E. Schmidt College of Medicine and was accepted in partial fulfillment of the requirements for the degree of Master of Science.

SUPERVISORY COMMITTEE:

Jangyenwu (Jul 20, 2021 13:59 EDT)

Jang Yen Wu, Ph.D.
Thesis Advisor

Howard M. Prentice (Jul 20, 2021 14:03 EDT)

Howard Prentice, Ph.D.

Rui Tao (Jul 21, 2021 14:24 EDT)

Rui Tao, DVM. Ph.D.

Janet Robishaw (Jul 22, 2021 14:53 EDT)

Janet Robishaw, Ph.D.
Chair, Biomedical Science

Sarah K. Wood M.D. (Jul 23, 2021 09:14 EDT)

Sarah K. Wood, M.D.
Interim Dean, Charles E. Schmidt College of Medicine

Robert W. Stackman Jr. (Jul 23, 2021 09:24 EDT)

Robert W. Stackman Jr., Ph.D.
Dean, Graduate College

July 23, 2021

Date

ACKNOWLEDGEMENTS

Thanks to the three members of his committee, Dr. Jang-Yen Wu, Dr. Rui Tao and Dr. Howard Prentice for their guidance, mentorship, and continued support throughout the research process. Dr. Jigar Modi, Dr. Yoshimi Shibata, Estaban Velasquez Saldarriaga and Subash Bhandari contributed to the experiments featured in this thesis. Dr. Janet Menzie, Dr. Lisa Ann Brennan, and Hongyaun Xu offered valuable technical advice throughout the research process. Ana Ritchie and Wen Ow helped to review this thesis.

Thanks to my academic advisor Dr. Bridget Smith who has been my invaluable guide through this program. Special thanks to Dr. Patricia Louis who encouraged me to choose this program and go on to medical school.

I would like to also thank my mother, father, sister, brother and friends for supporting me through many years of education. Lastly, I would like to thank Wen Ow for her partnership throughout this program.

ABSTRACT

Author: Zachary Lee

Title: GCSF GENE THERAPY FOR PARKINSON'S DISEASE

Institution: Florida Atlantic University

Thesis Advisor: Jang-Yen Wu Ph.D.

Degree: Master of Science

Year: 2021

The kynurenine pathway plays a critical role in regulating immunological homeostasis in the brain. Evidence supporting the hypothesis that kynurenine pathway dysfunction may exacerbate progression of neurodegenerative diseases like Parkinson's is growing. First, we investigate the effects of Interferon-γ, Lipopolysaccharide, and Interleukin-4 on several key kynurenine pathway metabolites using high performance liquid chromatography. We found that Interferon-γ had significant effects on the extracellular concentration of kynurenine metabolites in astrocytes, microglia, and macrophage. GCSF gene therapy is previously demonstrated to exert neuroprotective effects on models of Parkinson's and Alzheimer's disease. Seven days after receiving GCSF gene therapy, A53T Parkinson's mice were found to have increased levels of GCSF and tyrosine hydroxylase positive neurons. A concurrent increase in expression of the kynurenine pathway enzyme kynurenine aminotransferase 2 was observed. GCSF gene therapy may exhibit neuroprotective effects in a Parkinson's disease mouse model by restoring this key kynurenine pathway enzyme.

DEDICATION

This manuscript is dedicated first to Japo Pennycooke and Ken Lee. who both suffer from currently uncurable brain diseases. Then to their primary caretakers, Karen, Valerie, Joanne and Savanna whose selfless care of my grandparents represents the best of humanity.

GCSF GENE THERAPY FOR PARKINSON'S DISEASE

TABLES

FIGURES

CHAPTER 1: INTRODUCTION

Parkinson's disease is the second most common neurodegenerative disease affecting 1% of the population over the age of 60.[1] The loss of dopaminergic neurons in the substantia nigra pars compacta is a key pathological finding of Parkinson's disease along with aggregation of misfolded protein. Degeneration in the midbrain is the presumed cause of PD's characteristic motor and nonmotor symptoms.[2–4] However, many of these symptoms are not unique, rather they are shared among a host of neurodegenerative diseases including Alzheimer's and Huntington's disease. These similarities in both pathology and clinical presentation demonstrate a need to understand the disease not just for treatment of this condition but for a range of neurodegenerative conditions. First, we focus on further understanding how different stimuli can affect the kynurenine pathway, a growing area of focus in brain research. Secondly, we investigate the neuroprotective effects of human Granulocyte-Colony Stimulating Factor (hGCSF) gene therapy on a mouse model of Parkinson's disease.

1.1 Symptoms of Parkinson's disease

Bradykinesia, a slow initiation of voluntary movement is usually the first symptom present in Parkinson's disease. Often at the same time, muscular rigidity, a resting tremor and postural instability may be diagnosed. Patients with more advanced Parkinson's disease often have a stooped body posture and a shuffling gait that may lead to a loss of

balance and falls. Non-motor symptoms of Parkinson's disease include apathy, insomnia, dementia, and anxiety.[3–5]

1.2 Pathological Hallmarks and Therapies for Neurodegenerative Disease

There are several key pathological and molecular features that develop through the course of Parkinson's disease. Misshapen proteins associate with cognitive decline and loss of neurons in many neurodegenerative diseases. In Parkinson's disease, α-synuclein aggregates form primarily in the substantia nigra pars compacta and appear to associate with a loss of dopaminergic neurons. Under normal conditions, these neurons project to the basal ganglia where they synapse in the striatum's two parts, the putamen and caudate nucleus (**Figure 1**). The loss of these neurons in the nigrostriatal pathway explains some of the motor symptoms of the disease. Aggregates that form within neuronal perikarya are called lewy bodies, those inside neuronal processes are called Lewy neurites.[6]

The significance of protein aggregates is shared by other neurodegenerative disorders. In Multiple Systems Atrophy, α-synuclein plaques may form within oligodendroglial cells.[7] This leads to atrophy of the brain in a fashion that is similar to that seen in Parkinson's disease. In Alzheimer's disease hyperphosphorylated tau and clusters of extracellular amyloid-β preceded neuronal degeneration. In both Parkinson's and Alzheimer's disease, the association between protein aggregation, onset, and severity of pathological symptoms is less than perfect.[8,9] In fact, while certain drugs may reduce amyloid burden in AD patients, scant evidence exists for improvement of any symptoms.[10] In a recently approved antibody therapy for Alzheimer's disease, Aducanumab, PET scans confirmed that amyloid-β deposits were reduced after treatment. However only one of the two randomized controlled trials touted a significant effect

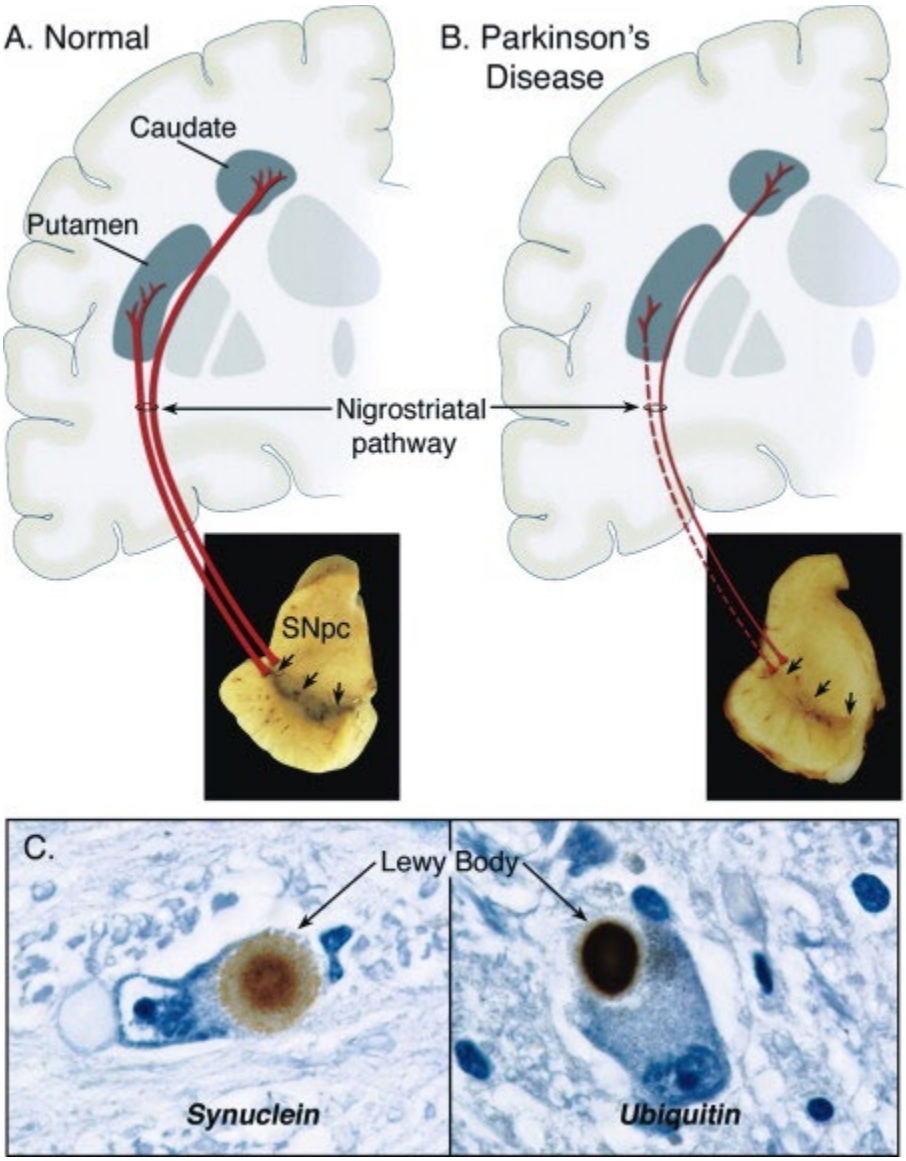

Figure 1. *Nigrostriatal dysfunction in Parkinson's Disease. A/B. Nigrostriatal pathway in healthy and diseased brain. The red line represents dopaminergic neuron projections C. Lewy bodies found within dopaminergic neurons in the Substantia Nigra pars compacta. Reused with Permission (Dauer W, Przedborski S. Neuron. 2003).*[6]

on the Clinical Dementia Rating, Sum of Boxes test. Neither study presents an association between the reduction of amyloid beta and reduced progression of dementia.[11,12] While little progress has been made in treating Alzheimer's disease patients, far more progress has been made at treating symptoms of Parkinson's disease. Upon recognition that dopamine neurons and subsequently, a loss of nigrostriatal

dopamine exacerbates disease progression, disease treatment has centered around dopamine metabolism. No drug more central to this pathway than levodopa, the immediate precursor to dopamine first shown to be efficacious in Parkinson's disease in the 1960s.[13]

Levodopa can cross the blood brain barrier where it is metabolized into dopamine by aromatic L-amino acid decarboxylase (AADC). Levodopa, often given with carbidopa to deliver it more efficiently to the brain treats many of the motor symptoms of Parkinson's disease. Other treatments that focus on the dopamine system are dopamine agonists, monoamine oxidase B (MAO-B) inhibitors and Catechol-O-methyl transferase (COMT) inhibitors. Together, these drugs increase dopamine concentrations or potency in the brain alleviating many of the motor symptoms of Parkinson's Disease. Importantly, these drugs only slow the progression of degeneration and symptoms reiterating the need for the discovery of novel therapies.[14–16]

1.3 The Kynurenine Pathway

The kynurenine pathway has been implicated in Parkinson's disease and many other neurodegenerative diseases.[17] The pathway begins with the ingestion of the essential amino acid L-Tryptophan. The unique albumin binding properties of L-tryptophan prevents 90% of plasma tryptophan from crossing the blood-brain barrier (BBB). The unbound 10% is free to be transported across the BBB by a competitive transporter along with other large neutral amino acids. Cerebral microvasculature around the BBB may also enhance the separation of tryptophan from albumin.[18]

The exact uptake mechanism of tryptophan from extracellular fluid into cells of the brain is unknown. While small portion of this tryptophan is taken up by serotonergic neurons to

begin the process of producing serotonin most of the extracellular tryptophan will be taken up by several non-neronal cells, namely astrocytes and microglia but also infiltrating macrophage and dendritic cells. In the periphery tryptophan 2,3-dioxygenase (TDO) is enzyme primarily responsible for the conversion of tryptophan to kynurenine. In the CNS, Indoleamine-2,3-dioxygenase (IDO) 1 and 2 primarily fulfills this role.[18] The fate of newly formed kynurenine likely hinges upon the type of cell that produced it (See a schematic of the kynurenine pathway **Figure 2**).[19] In microglia, kynurenine is transformed through a series of intermediates including anthranilic acid, 3-hydroxykynurenine, 3-hydroxyanthranilic acid and eventually quinolinic acid. Alternatively, in astrocytes, kynurenine is metabolized into kynurenic acid by kynurenine aminotransferase.

Kynurenine aminotransferase (KAT) has four known isoforms (numbered 1-4).[20,21] Kynurenine aminotransferases are found in the liver, skeletal muscles, and brain. KAT2, KAT3 and KAT4 localize to the mitochondria. Endurance exercise enhances KAT expression in individual skeletal muscle fibers.[22] KAT2 is responsible for 70% of kynurenic acid production in the brain.[23] A recent paper has noted that due to the kinetic properties of KAT1 and the in-vivo availability of the substrate kynurenine, it is more likely KAT1 uses glutamine as a substrate.[24] Several inhibitors of KAT2 have been identified.[23] One inhibitor of KAT2, glycrrhizic acid is noted to be highly selective for KAT2.[25] Kynurenic acid is typically present in the rat brain in picomole/mL[26] or picomole/gram of wet tissue[27] concentration. Kynurenic acid is a competitive antagonist of glycine at NMDA receptors and at α7 nicotinic acetylcholine receptors although the

latter claim is disputed.[28–30] The mechanism for kynurenic acid release from astrocytes is unknown.[30]

1.4 The Kynurenine Pathway in Parkinson's Disease

Inflammation is thought to exacerbate neurodegeneration. In Parkinson's disease, astrocytes and microglia congregate around the substantia nigra pars compact. Mouse studies have showed that preventing microglia from activating can decrease the severity of degeneration.[31] In addition to inflammation in the brain, a study in humans found that inflammation in the guts of PD patients was associated with elevations in Glial Fibrillary Acidic Protein and another marker of astrocytes.[32] Several mechanisms describing the anti-inflammatory properties of kynurenic acid have been described. Kynurenic acid in the high micromolar levels (>100 μM) can scavenge free radicals which may prevent further activation of microglia.[33] Kynurenic acid is shown to bind to G protein coupled receptor 35 which is present mostly on immune cells which also suggests it may directly interface with other immune cells.[34]

The alternate metabolite of kynurenine is quinolinic acid. When quinolinic acid is administered to mice, it can produce Parkinson's like symptoms. Additionally, it produces a main pathological hallmark of Parkinson's disease, α-synuclein like aggregates.[35] Quinolinic acid can also disrupt cytoskeletons, induce oxidative stress and activate microglia. Astrocytes but not neurons, can be induced to increase kynurenic acid after quinolinic acid stimulation suggesting some feedback mechanism.[33]

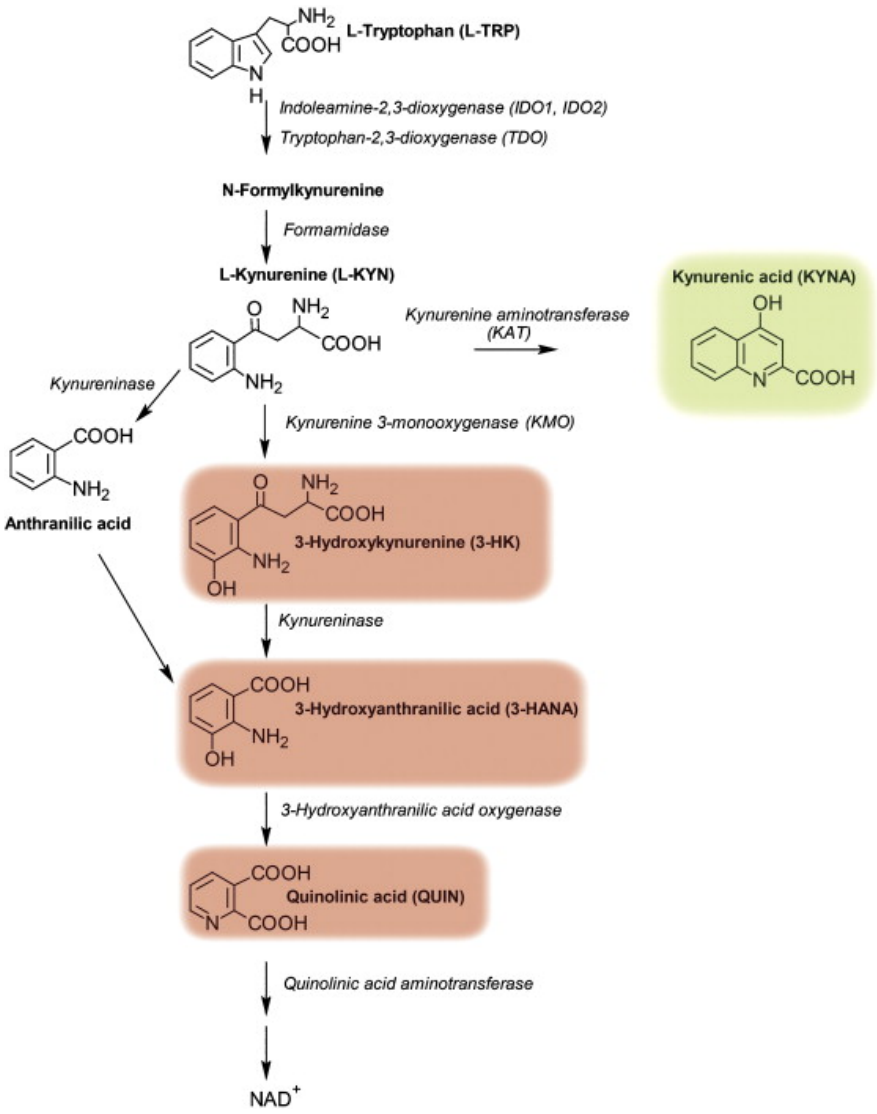

Figure 2. *Schematic Overview of the Kynurenine Pathway. Reused with permission (Maddison DC, Giorgini F. Seminars in Cell & Developmental Biology. 2015).*[19]

Kynurenic acid has known effects in other, non-neurodegenerative diseases of the CNS, such as depression. In unmedicated clinically depressed patients, the ratio of kynurenic acid to quinolinic acid in the blood is positively correlated with hippocampal and amygdalar volume.[36] Abnormal hippocampal neurogenesis has recently been reported in Parkinson's disease.[37] As depression and Parkinson's disease are common comorbidities[38] it is not surprising that there are ties between the two. This could have

implications in Alzheimer's disease where loss of hippocampal volume is associated with progression of the disease.[39]

Microglia, infiltrating macrophage, and astrocytes play complex and often dueling roles in the pathology of brain disease and injury. In traumatic brain injury models, microglia and macrophages migrate to the site of damage and release pro-inflammatory cytokines to orchestrate healing and prevent further damage. With increasing age however, microglia become 'primed' in such a way that makes pro-inflammatory responses more easily inducible.[40] One key function of microglia and macrophages is phagocytosis which involves the "eating" of a pathogen or debris. Upon contact with pathogens or cellular debris, these cells release reactive oxygen species. Stimulation of these immune cells may induce the release of other cytokines which in turn recruits other immune cells. In one model of neurodegenerative disease, the ensuing heightened reactivity of area immune cells may be a contributing factor in disease progression.[40–43]

The role of immune cells in neurodegenerative disease remains poorly understood. In Alzheimer's disease, accumulating amyloid-β plaques and tau proteins induce innate glial activation causing an increase in proinflammatory cytokines. This leads to more glial activation and unfortunately, also increases the rate of amyloid-β aggregation, initiating a positive feedback loop that leads to runaway inflammation.[40,44,45] It is unclear why microglia activation might exacerbate amyloid-β deposit formation. In addition, the presence of amyloid-β plaques near free radicals may catalyze the production of more amyloid-β without cellular intervention.[46] Some studies report that amyloid-β can form in the absence of microglia complicating this intererpretation.[47] When lipopolysaccharide, a common inflammatory molecule, is injected into the substantia nigra of rats with

ulcerative colitis a disease of peripheral inflammation, Tumor Necrosis Factor-α (TNF-α), Interleukin-1β (IL-1β), and Interleukin-6 (IL-6) were elevated, proliferation of microglia and astrocytes, and loss of dopaminergic neurons was observed.[48]

Still, evidence suggests that glia can be recruited to remove amyloid-β without worsening the disease. IL-6 and IL-1β are key cytokines involved in both PD and AD. IL-6 was elevated in the cerebrospinal fluid but not plasma of patients with both diseases.[49] Upregulation of the IL-6 gene into two different mouse models of Alzheimer's disease caused microglia to phagocytose amyloid-β at a rate high enough to reduce amyloid-β plaque formation. Interestingly, the increased amyloid-β uptake did not cause microglia to further worsen the amyloid beta load despite undergoing gliosis.[50] That study indicates that in AD, IL-6 may activate microglia without the accompanying inflammation that results in amyloid-β aggregation. Under normal physiological conditions IL-6 causes astrocytes to release nerve growth factor which promotes neuron differentiation.[51]

Interestingly, primary cultures of human astrocytes were reported to increase expression of GCSF when stimulated with Interferon-γ (IFNγ) and IL-1β or TNF-α.[52] The same authors reported that stimulation of astrocytes with IL-1β and TNF-α caused increased levels of IL-6 mRNA and protein. Interpreting the different effects of IFNγ on immune cells of the brain is complicated by various factors. For instance, IFNγ receptor is found to be overexpressed in microglia in cell culture compared to microglia in healthy, AD, and PD brain tissue.[53]

1.5 Granulocyte Colony Stimulating Factor Gene Therapy

Granulocytes are white blood cells that have broad functions in initiating immune response to infection and repairing damaged tissue. Drug analogs of human GCSF have

been used to replenish neutrophils lost by patients undergoing chemotherapy. In the last decade, GCSF has been shown to have neuroprotective properties. In stroke models, GCSF increased hematopoietic stem cells in the brain, reduced endoplasmic reticulum stress, improved vascularization, and promoted the growth of new neurons.[54–56] In another stroke model, GCSF activated the mTOR/p70S6K pathway leading to reduced expression of inflammatory cytokines including IL-1β and TNF-α.[57] The rho kinase inhibitor Fausdil was able to promote neurogenesis in part by inducing astrocytes to induce GCSF production.[58] In a Parkinson's disease mouse model, subcutaneous GCSF increased expression of dopaminergic neurons.[59] Notably, astrocytes and glia were found to be significantly increased in the striatum and hippocampus in the GCSF group.[40] In an Alzheimer's mouse model, GCSF treated mice had increased levels of α7 nAChR protein and decreased pro-inflammatory cytokines including IL-6.[60] Previously, transgenic Alzheimer's mice have also been shown to perform better in radial arm maze tests, and have reduced amyloid-β plaques after GCSF was administered.[54]

Interestingly, there has been some debate within the literature about which cells express GCSF and GCSF receptor. Initially, work in the early 1990s showed that astrocytes could produce GCSF after incubation with TNF-α or IL-1b. In 2005, immunohistochemical analysis of rat brains showed no localization with glial fibrillary acidic protein with GCSF but strong localization with neurons.[61] However, a recent systematic study found that while GCSF and its receptor is mostly localized in neurons, it was also found in other cell types including epididymal cells, cells of the choroid plexus and most notably, astrocytes.[62] That study found no difference in the distribution of GCSF or its' receptor in the brains of AD patients suggesting that it does not play a causal role in the disease.

1.6 Cell Culture Background

Immortal cell lines have significant advantages, they are inexpensive, relatively easy to assay, and have few ethical concerns compared with primary cells. But challenges remain for responsible use of immortal cell lines. One study of a cell line library estimated that over one third of submissions were contaminated. The most common contaminant by far was Mycoplasma, which is resistant to most common antibiotics and is impossible to detect with standard microscopy.[63] The hardiness of mycoplasma is hard to understate. In one experiment, a mycoplasma free culture was subcultured weekly in a fume hood infected with mycoplasma. In 6 weeks, the culture tested positive for mycoplasma.[64]

In order to prevent contamination, strict aseptic technique will be followed. This includes sterilizing surfaces of the laminar fume hood with UV light treatment and 70% ethanol before use. All items passed into the hood will also be sprayed with 70% ethanol. The culture dish will remain sealed until it is within the sterilized fume hood. In addition, gloves will be worn when handling cell cultures which will be frequently coated with 70% ethanol to help prevent contamination.[65]

1.7 Mouse Models of Parkinson's Disease

While no animal model can perfectly recapitulate the complex biochemical and symptomatic features of Parkinson's disease, their use may yield valuable insights with fewer ethical implications than when working with higher mammals. Parkinson's like symptoms and pathology can be induced through genetic manipulation or chemical administration.

The modern landscape of Parkinson's mouse models arguably began with the discovery of Parkinson's like symptoms in students who had mistakenly synthesized and then self-

administered 1-methyl-4-phenyl-1,2,3,6-tetrahydropyridine (MPTP).[66] A treating physician, Dr. J. William Langston, recognizing the possible value of this treatment attempted to establish a model using intraperitoneal administration of MPTP to squirrel monkeys. In his experiments he noted dramatic cell loss of the substantia nigra, very closely mirroring that loss seen in patients with Parkinson's disease.[67] Further experimentation showed that MPTP could induce many of the motor symptoms of Parkinson's disease and other groups translated this research to mice.[68]

MPTP mice gradually became one of the dominant models of Parkinson's disease. MPTP, which is not neurotoxic by itself becomes so when converted to 1-methyl-4-phenylpyridium(MPP+) by astrocytes with MOA-B in the brain. MPP+ is taken up selectively by dopamine neurons by dopamine transporter (DAT). Once inside the dopamine neuron, MPP+ inhibits mitochondrial respiration leading to a remarkable decrease in ATP in the substantia nigra pars compacta. The resulting dopamine neuron degeneration occurs over a period of about a week although this varies significantly with age.[69,70] One critical drawback of MPTP mice is the lack a PD hallmark, Lewy bodies.[66] A less common chemically induced Parkinson's mouse model, 6-hydroxydopamine (6-OHDA), shares similar patterns of neurodegeneration in the Substantia Nigra pars Compacta as the MPTP model. Upon direct injection to the Substantia Nigra pars Compacta, the 6-OHDA, forms reactive oxygen species and triggers degeneration resulting in some motor impairments. Like the MPTP model, Lewy bodies do not form.[71]

As the genes linked to cases of familial Parkinson's Disease were uncovered, the race to develop a genetic model took off. One such gene, alpha-synuclein, is present in the presynaptic terminals of healthy neurons. In patients with the A53T point mutation in the

alpha-synuclein gene, alpha-synuclein forms a major component of Lewy bodies.[71] Mouse models that knockout the alpha-synuclein gene are protected against MPTP.[72] Mouse models that overexpress A53T mimic the lewy body pathology observed in Parkinson's disease. Dopamine neurons are also reduced in the striatum, but interestingly not in the substantia nigra as observed in Parkinson's disease.[73–75]

A53T mice do show changes in motor performance including arched back, severe muscle weakness, and ataxia approaching 1 year of age.[76] Non-motor changes in A53T mice also recapitulate Parkinson's disease with hyperactivity, reduced anxiety, loss of olfaction and depressive like behaviors.[77–79]

CHAPTER 2: METHODS

2.1 Cell Culture Cytokine/Lipopolysaccharide Stimulation

Since different cell types are reported to have vastly different roles in producing tryptophan metabolites, we designed an experiment to stimulate cells with cytokines or lipopolysaccharide and quantify the extracellular metabolites. We used A172 cells to represent astrocytes, HMC3 cells to represent microglia, and RAW264.7 cells to represent macrophage. Each cell type was seeded at 1-2 x 10^6 $\frac{cell}{ml}$ in 6 cm culture dish with their respective media (**Table 1**).

Cell Type	Media	Additives
A172	Dulbecco's Modified Eagle's Medium	10% Fetal Bovine Serum 1% Penicillin/Streptomycin
HMC3	Eagle's Minimum Essential Medium	
RAW 264.7	Dulbecco's Modified Eagle's Medium	

Table 1. *Description of media used during the cytokine/lipopolysaccharide stimulation experiment.*

Cells were incubated overnight at 37˚C and 5.5% CO_2 to allow adherence to the plate. Then either IFNγ, LPS, IL-4 or saline was added to each well at a concentration at $20\frac{ng}{ml}$ except for saline in which 10µl was added. After 24 hours of incubation, media was collected for HPLC analysis and stored in -80ºC freezer. Upon thawing, 5% perchloric acid was added to each tube and it was centrifuged at 25,000 RCF for 30 minutes. The supernatant was collected and used for HPLC analysis.

2.2 Parkinson's Mice

A53T αSyn wild type (Wild Type) and transgenic B6;C3-Tg(Prnp-SNCA*A53T)83Vle/J (Parkinson's disease) mice were raised in the Florida Atlantic University Vivarium under standard conditions. These mice represent a Parkinson's disease pathological phenotype of over expressed α-synuclein on neurons.[84,85]

Mice received either no eye drop, GCSF gene therapy (AAV-CMV-GCSF $3x10^9$ PFU in 1.5uL), or vector gene therapy (AAV-CMV-GFP $3x10^9$ PFU in 1.5uL) in the left eye. Mice were sacrificed 7 days after gene therapy.

2.3 RNA Extraction and RT-PCR

Reverse Transcription Polymerase Chain Reaction (RT-PCR) quantifies the expression of a particular gene. It involves three main parts, extraction of RNA from a tissue, amplification of the target RNA, and quantification of each amplicon.

Brain tissue was harvested using a mouse brain matrix and cut into 2 mm sections from the frontal lobe. The left side of the brain was used for RNA analysis. Total RNA was extracted using the RNeasy Mini Kit without deviation from instructions. DNA was removed using Turbo DNase (Thermo Fisher Scientific). Random pd(N)6 primer and Thermoscript RT-PCR system (Life Technologies) were used to reverse transcribe extracted RNA. The housekeeping gene Actin was used to normalize expression. Samples were amplified and quantified with the Alilent Aria Mx real time PCR system using SYBR green dye. Analysis was conducted with Aria Mx 1.5. Primers used can be found in (**Table 2**).

Gene	Primer Direction	Sequence
Human Granulocyte-Colony Stimulating Factor [80]	Forward	5'-AACTCGGGGGAGATCCCTTCCA-3'
	Reverse	5'-ACTCTCTGGGCATCCCCCT-3'
mTyrosine Hydroxylase (TH)	Forward	5'-TGTTGGCTGACCGCACAT-3'
	Reverse	5'-GCCCCCAGAGATGCAAGTC-3'

Table 2. *Description of primers used in Reverse Transcriptase PCR experiment.*

2.4 Protein Extraction and Western Blot

After sacrifice, the whole brain was dissected out and divided into both a frontal (0-4mm) 'R1' and middle 'R2' section (4-8mm). The frontal R1 section contains parts of the cerebrum including the cerebral cortex and early parts of the striatum. The middle R2 contains some cortex, importantly the part of the striatum that includes the caudate putamen, and part of the reticular region of the substantia nigra. For a more details of the dissected area view (**Figure 3**). The tissue was snap frozen in liquid nitrogen until ready to be processed. Brain tissue was weighed and submerged in proportional volume of RIPA buffer with 1% phosphatase and 1% protease. Tissue was homogenized with a Branson Digital Sonifier. Each sample received two 7 second long pulses separated by 3 minute incubation on ice. After vortexing, an aliquot of each sample was collected and subjected for the Bicinchoninic Acid Assay (BCA) for protein while the remaining samples returned to the -80°C freezer.

The BCA assay estimates the total amount of protein in each sample. First a dilution solution of 90% water and 10% RIPA is created to mimic the solution used in our tissue collection protocol. A bovine serum albumin stock is dissolved in the dilution solution. Then serial dilutions were performed to achieve standards through the anticipated linear range of the assay 0.5-0.05$\frac{mg}{ml}$. The BCA reagent was diluted to the working

concentration. In each well, 200uL BCA working solution and 10uL sample or standard is loaded in triplicate. The absorbance is read on a microplate reader at 595 nm. Standard curves were accepted when $R^2 \geq 0.97$.

Western blotting relies on three main mechanisms. First, an electrical current separates protein in a sample by size in on a sodium dodecyl sulfate polyacrylamide gel. This gel is formulated with reducing agents to degrade sulfhydryl groups and disulfide bonds while leaving the primary protein structure intact. The gel is made of two parts, a stacking component that enables wells for protein to be loaded and a separating component that separates the proteins by molecular weight. The recipe for the SDS-polyacrylamide gel used in these experiments is found in (**Table 3**). The electrophoresis step adds additional specificity compared to other antibody dependent protein assays such as enzyme linked immunoassays. 100ug of protein were loaded into each lane. Each gel ran for 90 minutes at 150 volts.

	12% Separating Gel	6% Stacking Gel
Distilled Water	10.2 mL	8.7 mL
40% Acrylamide	7.2 mL	2.25 mL
1.5 M Tris pH 8.8	6 mL	0 mL
0.5 M Tris pH 6.8	0 mL	3.75 mL
10% Sodium Dodecyl Sulfate	240 uL	150 uL
TEMED	24 uL	15 uL
10% Ammonium Persulfate	240 uL	150 uL

Table 3. *Ingredients used for the sodium doedecyl sulfate polyacrlamide gel which is used to separate protein by size prior to a western blots.*

The next step involves transferring the proteins from the gel to a nitrocellulose membrane. To do this, a transfer sandwich was made. The sandwich was loaded into the cassette and run at 30 volts for 90 minutes in transfer buffer. Following the transfer, the

nitrocellulose membrane was briefly incubated with ponceau stain to confirm a successful separation and transfer.

After washing with Tris Buffered Solution with Tween (TBST) to remove all remaining ponceau's stain, the membrane was soaked in a 2.5% nonfat milk TBST solution for 1 hour. This blocking step prevents nonspecific protein-antibody interactions. Next, proteins on the membrane are exposed to a primary antibody specific to the protein of interest diluted in 1.5 mL of TBST. Then a secondary antibody coupled with a fluorescent enzyme binds to the primary antibody and the membrane is imaged with a Licor Odyssey Fc Imaging System. For a list of antibodies used, see (**Table 4**). The Odyssey exposes the membrane to 600 nm, 700 nm, and 800 nm light to stimulate fluorescence of the secondary antibody and the molecular weight ladder. Bands were identified and quantified with Image Studio Lite version 5.2.

Membranes were restriped by incubating with restriping buffer for 15 minutes, washing with TBST and repeating the experiment starting with the blocking step. The same membrane was restriped no more than three times to prevent loss of target or housekeeping protein.

In each lane of the western blot, we identified at least two proteins, the protein of interest, as well as a loading control GAPDH. Loading controls are expressed without much variation in a variety of tissues. Thus, the loading controls help account for differences in the amount of tissue loaded in each well. These differences may be caused by imprecise pipetting or the amount of tissue used per sample.

2.5 High Performance Liquid Chromatography

High performance liquid chromatography (HPLC) is a technique for analyzing the presence of chemicals in a liquid sample. Generally, a pump pushes the mobile phase through a tightly packed column known as the stationary phase. An analyte is injected into the mobile phase upstream of the column. When it reaches the column, chemicals in the sample are separated by their polarity due to their affinity to the beads in the column. As they leave the column, they pass a detector which gives a response readout that can be used to quantify the amount of compound present.

For detection of kynurenic acid, a Shimadzu RF-10AXL Fluorescence Detector with the PowerChrom 2.5.13 software was used for metabolite detection. For this metabolite a Shimadzu LC-10ADVP pumped through a 50 mm Sodium Acetate 10.0% Acetonitrile mobile phase at 0.6 mL/min. After the column a Wiz ISCO pumped Zinc Acetate at 0.5 mL/min. For tryptophan, kynurenine, anthranilic acid, and 3-hydroxy-anthranillic acid, the Waters 2996 Photodiode Array using Waters Empower 3 software was used in addition to the fluorescence detector. In this setup a monosodium phosphate 88.32 mM, disodium phosphate anhydrous 12.28 mM, 15% methanol mobile phase was pumped in at 0.6 ml/min. 10 µL of each sample was analyzed.

To make the standards, the pure metabolite was first dissolved in Dimethyl Sulfoxide 0.1 g of metabolite/100µL. Subsequent serial dilutions were performed with nanopure water to reach appropriate concentrations. The column was washed with nanopure water as well as 0.1 N Nitric acid. Standards were made fresh daily. For each of the kynurenine metabolite standard the $R^2 > 0.97$.

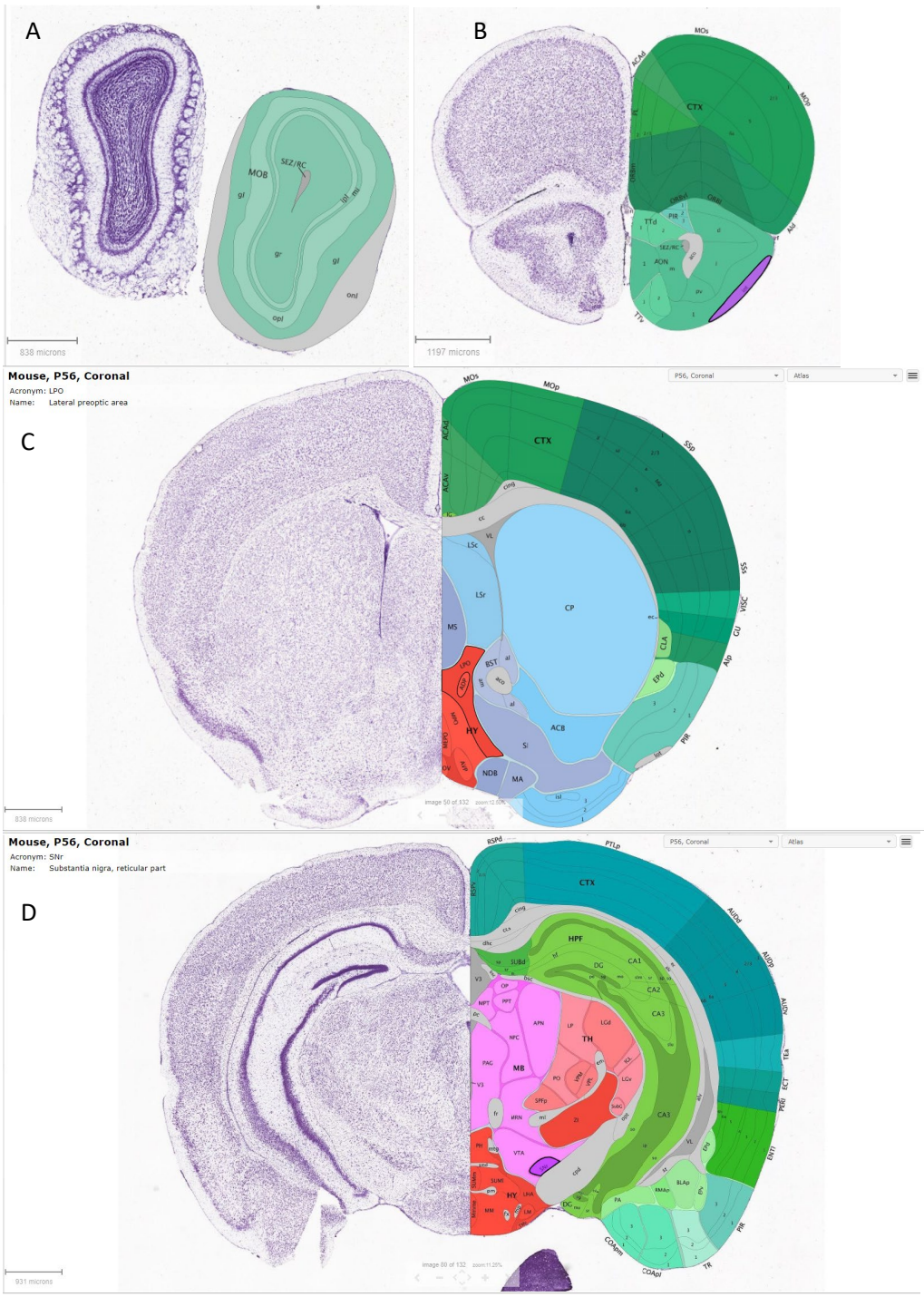

Figure 3. *Coronal slices of mouse brain representing structures found in dissected regions. A. Structures found in R1 slice 1mm from frontal pole including several cerebral cortex features B. Structures found in R1 slice 3mm from frontal pole including cerebral cortex features and early cerebral nuclei. C. Structures found in R2 slice 5mm from frontal pole including the caudate putamen. D. Structures found in R2 slice 8mm from frontal pole including the reticular region of the substantia nigra. Reused with permission from the Allen Mouse Brain Atlas. Image credit: Allen Institute.*[81]

Antibody	Manufacturer	Product # Lot #	Dilution	Molecular Weight
Rabbit pAB Kynurenine Aminotransferase 2	Rockland	600-401-J37 33473	1:200	49kDa
Rabbit mAB to Recombinant Granulocyte Colony Stimulating Factor	Abcam	Ab181053 GR3223080-3	1:2000	60kDa
Rabbit pAB to Tyrosine Hydroxylase	Abcam	Ab112 GR3244479-2	1:200	24kDa
GAPDH	Cell Signaling Technology	D16H11 5174S	1:5000	36kDa
LICOR	IRDye 800CW Goat anti-Rabbit	926-32211 C80925-25	1:10,000	n/a

Table 4. *Antibodies and dilutions used for western blot.*

CHAPTER 3: RESULTS

4.1 A172 Astrocytes

The media in which we cultured A172 astrocytes contained the amino acid tryptophan which explains why the media only condition had the highest level of tryptophan (**Figure 4**). Compared to the media only condition, the saline condition showed a significant reduction in the levels of tryptophan. LPS appeared to slow the degradation of tryptophan in the media although this effect was not statistically significant. IL-4 did not appear to affect the degradation of tryptophan. IFNγ nearly caused all of the tryptophan in the media to be depleted.

In the kynurenine pathway, tryptophan is transformed into kynurenine by IDO1, IDO2 or TDO. No kynurenine was detected in the media only condition (**Figure 5**). In the saline condition, an increase in kynurenine was detected. Compared to the saline group, IFNγ, LPS and IL-4 conditions saw an increase in kynurenine. A roughly 2-fold increase was observed in the IL-4 and LPS groups and a 10-fold increase in the IFNγ group.

Kynurenic Acid is one of the terminal products of the kynurenine pathway, resulting immediately from kynurenine. No difference in the amount of kynurenic acid was seen in the media only and the saline group (**Figure 6**). No difference was seen in the IL-4 or LPS groups. However, the IFNγ group saw a modest increase.

3-hydroxyanthranilic acid and anthranilic acid are other possible products in the kynurenine pathway. Anthranilic acid may form directly from kynurenine while 3-

hydroxyanthranilic acid may form indirectly from kynurenine through either anthranilic acid or 3-hydroxykynurenine. No statistically significant changes were observed in either metabolite however differences in the mean were noted that may indicate that changes did occur, but we did not have the statistical power to observe them (**Figures 7** and **8**).

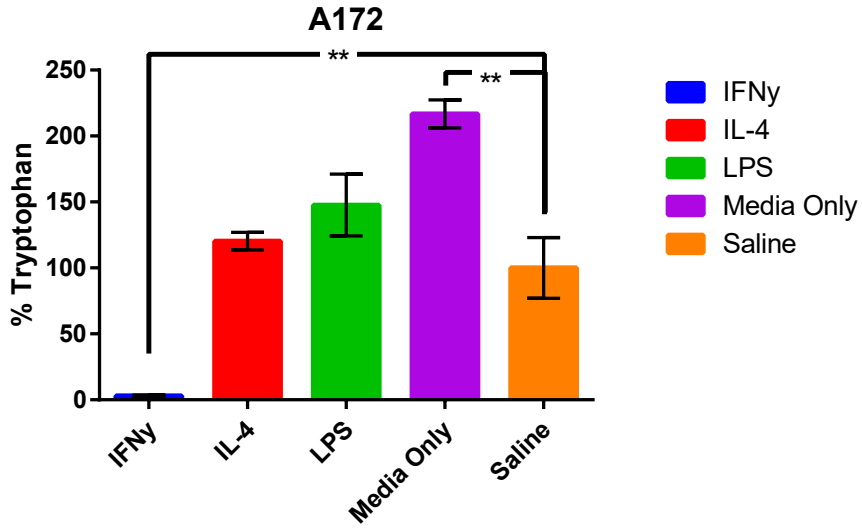

Figure 4 *A172 cells grown in Dulbecco's Modified Eagle Media 10% Fetal Bovine Serum were incubated for 24 hours with the above chemicals. The media was collected, processed and subject to HPLC to identify extracellular tryptophan. Tryptophan is present in sterile media without cells in high amounts. The saline condition resulted in significant reductions in the amount of detected extracellular tryptophan. Compared to the saline condition, IL-4 and LPS were statistically equivalent while IFNγ stimulation resulted in a remarkable reduction in availability of tryptophan. (n=6 Error bars represent the standard error of the mean)*

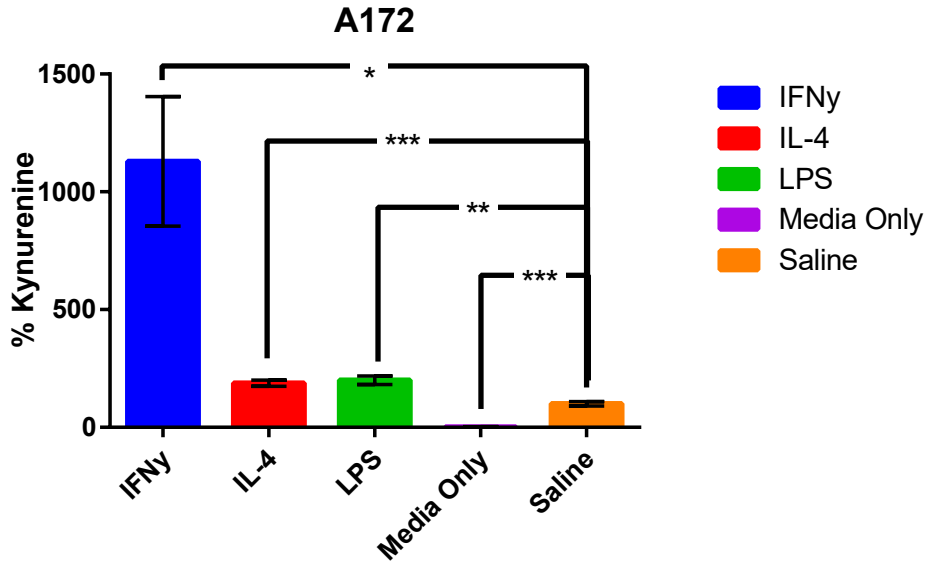

Figure 5. *A172 cells grown in Dulbecco's Modified Eagle Media 10% Fetal Bovine Serum were incubated for 24 hours with the above chemicals. The media was collected, processed and subject to HPLC to identify kynurenine. No kynurenine was detected in the sterile media without cells. The saline condition resulted in an increase in detectable kynurenine. Compared to the saline condition, IL-4 and LPS resulted in a rough doubling of extracellular kynurenine while the IFNγ condition dramatically increased extracellular kynurenine. (n=6 Error bars represent standard error of the mean)*

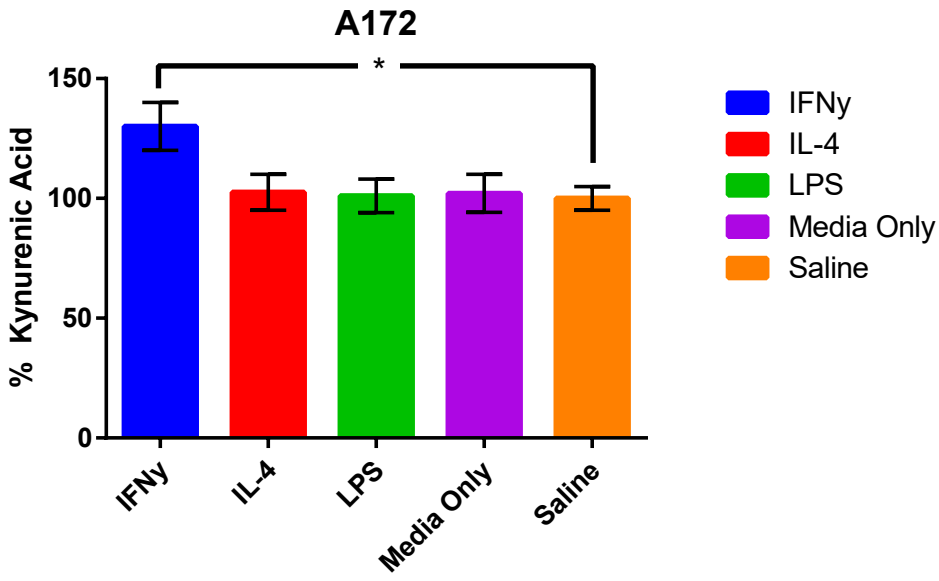

Figure 6. *A172 cells grown in Dulbecco's Modified Eagle Media 10% Fetal Bovine Serum were incubated for 24 hours with the above chemicals. The media was collected, processed and subject to HPLC to identify extracellular kynurenic acid. Stimulation with IFNγ resulted in an increase in kynurenic acid. IL-4, LPS, and media without cells did not result in changes in the amount of kynurenic acid present in the media. (n=6 Error bars represent standard error of the mean)*

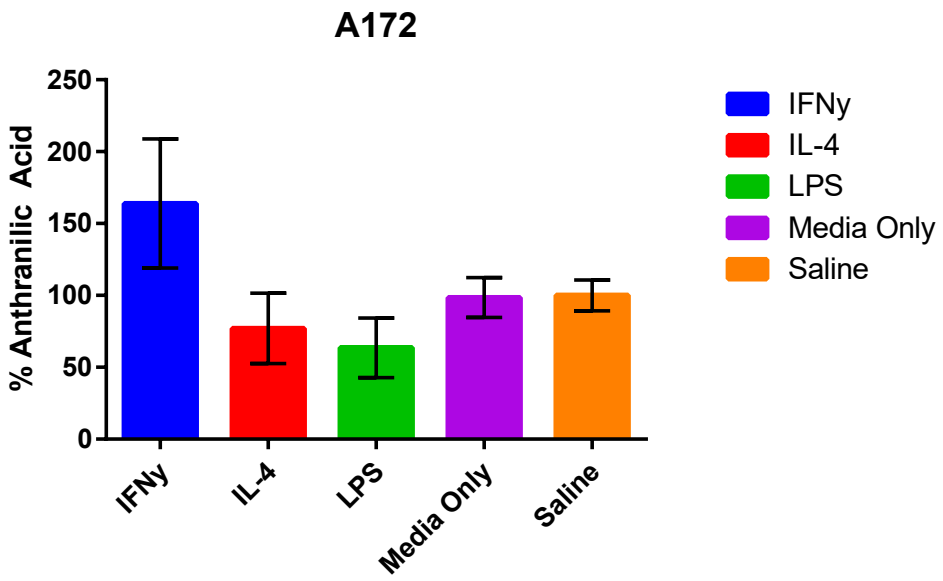

Figure 7. *A172 cells grown in Dulbecco's Modified Eagle Media 10% Fetal Bovine Serum were incubated for 24 hours with the above chemicals. The media was collected, processed and subject to HPLC to identify extracellular anthranilic acid. While no statistically significant observations were observed, the investigator believes that this is due to a lack of power as the mean anthranilic acid appeared to vary from the saline condition in the IFNγ, IL-4 and LPS groups. (n=6 Error bars represent standard error of the mean)*

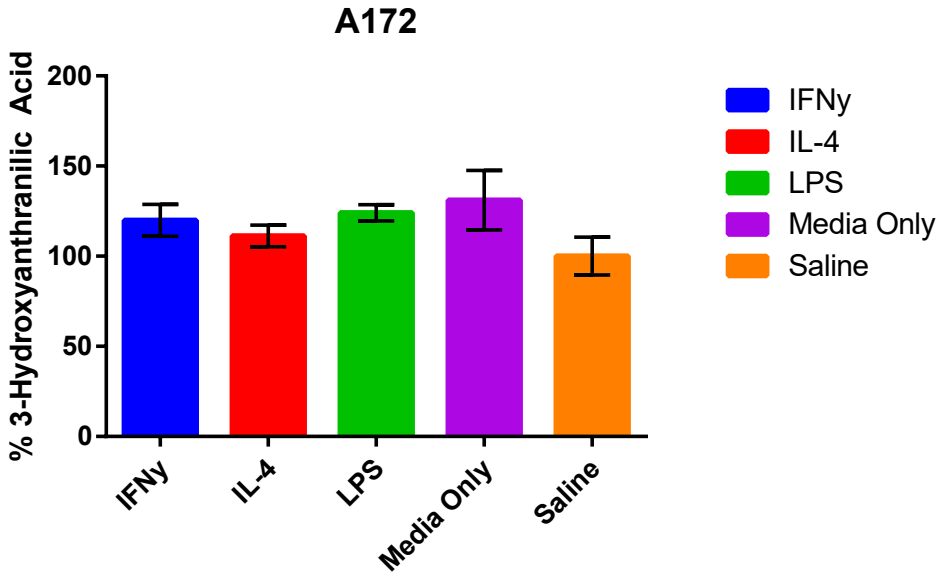

Figure 8. *A172 cells grown in Dulbecco's Modified Eagle Media 10% Fetal Bovine Serum were incubated for 24 hours with the above chemicals. The media was collected, processed and subject to HPLC to identify extracellular 3-hydroxyanthranilic acid. No significant changes to this metabolite were observed. (n=6 Error bars represent standard error of the mean)*

3.1 HMC3 Microglia

As in the A172 media, the HMC3 media contained the amino acid tryptophan. No differences were noted in the tryptophan levels of the saline, media only, LPS or IL-4 groups. However, IFNγ group saw a roughly 40% reduction in tryptophan levels compared to the saline group (**Figure 9**).

Kynurenine was not detected in the HMC3 media. No statistically significant differences in kynurenine were detected in any group. However, an increase in the mean kynurenine of the LPS and IFNγ groups were observed. Our investigation likely did not have the statistical power to resolve the differences that occurred (**Figure 10**).

No differences in Kynurenic acid were observed between each group and the saline condition (**Figure 11**). Measurement of 3-hydroxyanthranilic acid was lowest in the media only group. The saline group was approximately triple the media only group and statistically equivalent with the IL-4 and LPS conditions. The IFNγ condition had less 3-hydroxyanthranilic acid than the saline condition (**Figure 12**). No anthranilic acid was observed.

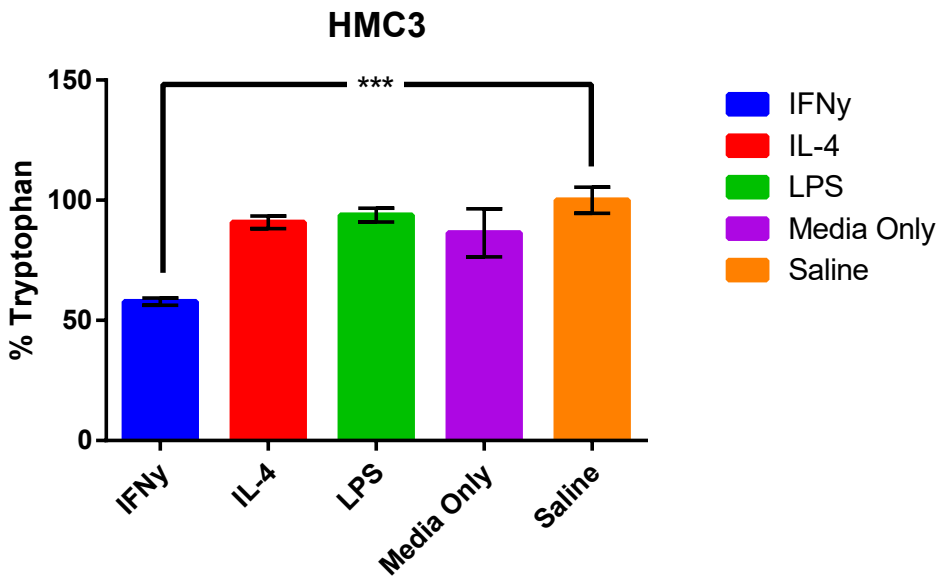

Figure 9. *HMC3 cells grown in Eagle's Minimum Essential Medium 10% Fetal Bovine Serum were incubated for 24 hours with the above chemicals. The media was collected, processed and subject to HPLC to identify extracellular tryptophan. Tryptophan is present in sterile media without cells. The saline, IL-4, and LPS conditions had equivalent amounts of tryptophan. Tryptophan was reduced in the IFNγ condition compared to the saline condition. (n=6 Error bars represent the standard error of the mean)*

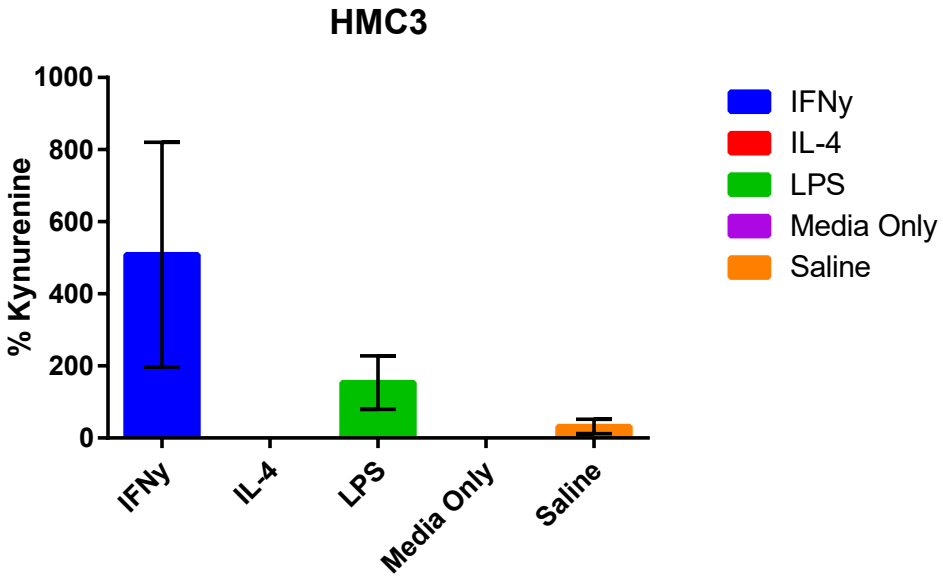

Figure 10. *HMC3 cells grown in Eagle's Minimum Essential Medium 10% Fetal Bovine Serum were incubated for 24 hours with the above chemicals. The media was collected, processed and subject to HPLC to identify extracellular kynurenine. No statistically significant differences were observed but compared to the saline group, the mean kynurenine was greater in the IFNγ and LPS group and decreased in the IL-4 group. (n=6 Error bars represent the standard error of the mean)*

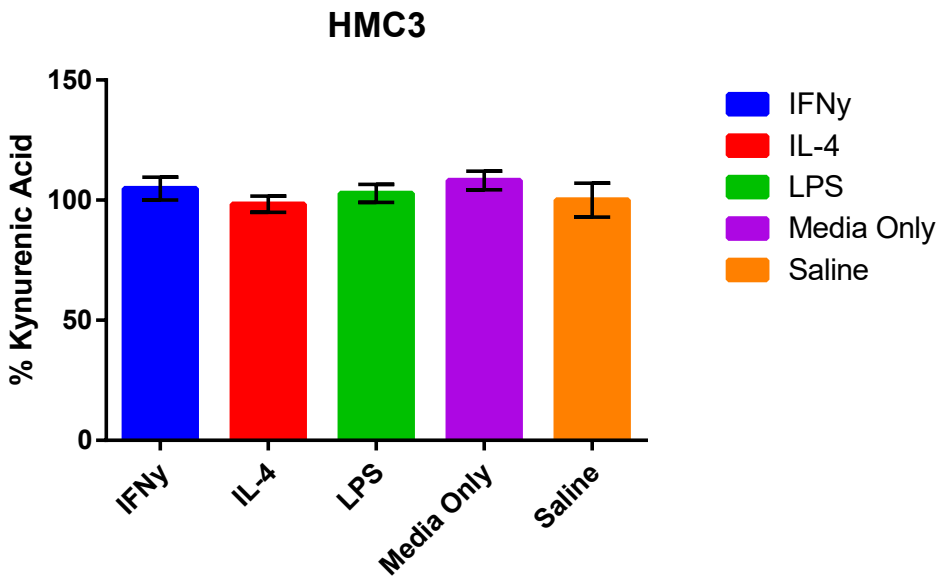

Figure 11. *HMC3 cells grown in Eagle's Minimum Essential Medium 10% Fetal Bovine Serum were incubated for 24 hours with the above chemicals. The media was collected, processed and subject to HPLC to identify extracellular kynurenic acid. No statistically significant differences were observed. (n=6 Error bars represent the standard error of the mean)*

3.1 Raw 264.7 Macrophage

As with the other two cell lines, the media of RAW 264.7 cells contained tryptophan that was depleted in each condition (**Figure 12**). The saline condition reduced the available tryptophan by about a third. The saline condition was statistically equivalent with the IL-4 and LPS conditions although visually did appear to be lower in the LPS condition. IFNγ had a higher amount of tryptophan indicating that it slowed the degradation of tryptophan.

No kynurenine, 3-hydroxyanthranilic acid, anthranilic acid, or kynurenic acid was detected in any of the Raw 264.7 macrophage samples (data not shown). P values from all HPLC experiments can be found in (**Table 5**).

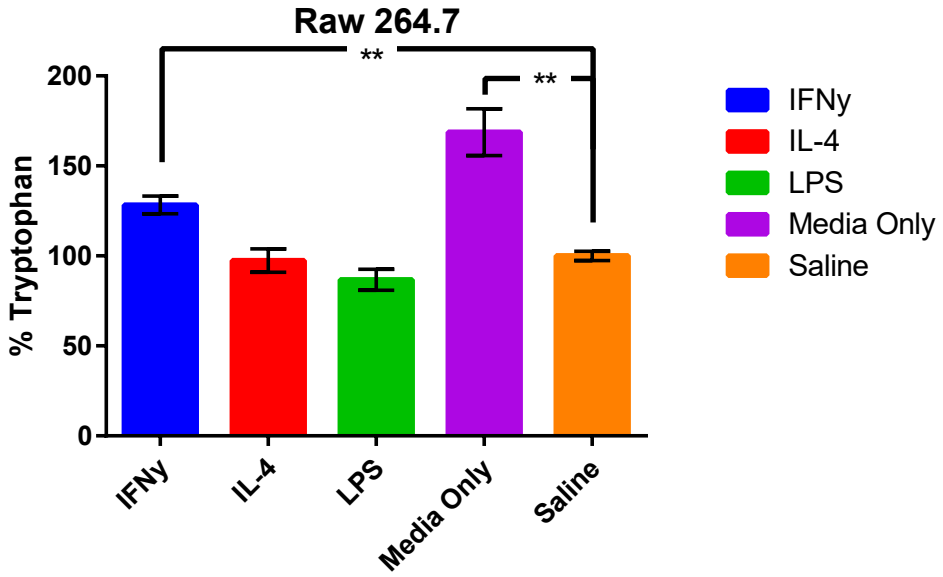

Figure 12 *Raw 264.7 cells grown in Eagle's Minimum Essential Medium 10% Fetal Bovine Serum were incubated for 24 hours with the above chemicals. The media was collected, processed and subject to HPLC to identify extracellular tryptophan. Tryptophan is present in the media only condition without cells at higher rates than the saline condition. (n=2 Error bars represent the standard error of the mean)*

		IFNγ vs Saline	IL-4 vs Saline	LPS vs Saline	Media Only vs Saline
A172	Tryptophan	** 0.0085	Ns 0.04315	Ns 0.1775	** 0.0025
	Kynurenine	* 0.0134	*** 0.0005	** 0.0012	*** 0.0001
	3-Hydroxyanthranilic Acid	Ns 0.1796	Ns 0.3816	Ns 0.0751	Ns 0.1495
	Kyunrenic Acid	* 0.0298	Ns 0.7868	Ns 0.9094	Ns 0.8267
	Anthranilic Acid	Ns 0.2192	Ns 0.4187	Ns 0.1594	Ns 0.9337
HMC3	Tryptophan	*** .0003	Ns .1675	Ns 0.3426	Ns .2670
	Kynurenine	Ns 0.1869	Ns 0.1747	Ns 0.1680	Ns 0.1747
	3-Hydroxyanthranilic Acid	Ns 0.3449	Ns 0.3449	Ns 0.3774	**** < 0.0001
	Kynurenic Acid	Ns 0.5894	Ns 0.8350	Ns 0.7374	Ns 0.3419
RAW 264.7	Tryptophan	** 0.0011	Ns 0.7220	Ns 0.0751	** 0.0028

Table 5. *P values from Welch's t test for unequal variances for kynurenine pathway metabolites measured in HPLC experiments.*

3.2 Detection of human-Granulocyte Colony Stimulating Factor Gene Therapy

To demonstrate that the hGCSF gene therapy increased expression of hGCSF in Parkinson's mice 7 days after delivery, we conducted RT-PCR and western blots on different sections of the brain. The wild type control and A53T mice that received the AAV-CMV-GFP vector had no differences in GCSF expression in the basal ganglia (**Figure 13**) or diencephalon (**Figure 14**). hGCSF expression increased 2-3 fold in the basal ganglia of A53T mice receiving AAV-CMV-hGCSF gene therapy compared to the vector control. hGCSF expression increased 3 fold in the diencephalon of A53T mice receiving AAV-CMV-hGCSF gene therapy compared to the vector control. These results indicate that AAV-CMV-hGCSF gene therapy successfully increases the level of hGCSF mRNA in two distinct parts of the A53T mice brain.

GCSF protein expression in the R1 forebrain region of the brain did not differ significantly from the WT control. GCSF protein expression in the R2 midbrain region of the brain was significantly higher in the GCSF gene therapy group compared to the other groups. (**Figure 15**)

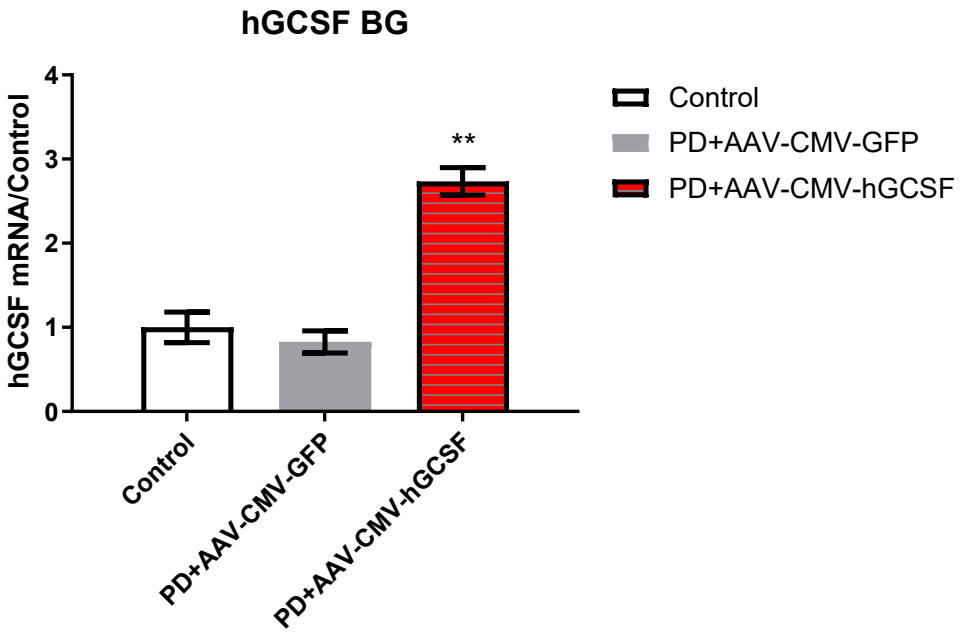

Figure 13. *qPCR quantification of hGCSF mRNA in the basal ganglia of Parkinson's disease mice 7 days after delivery of AAV-CMV-hGCSF gene vector via eye drop. PD mice treated with AAV-CMV GCSF show >2-fold change in expression of hGCSF mRNA compared to PD mouse treated with AAV-CMV-GFP on day 7. (n=2 Error bars indicate the standard error of the mean)*

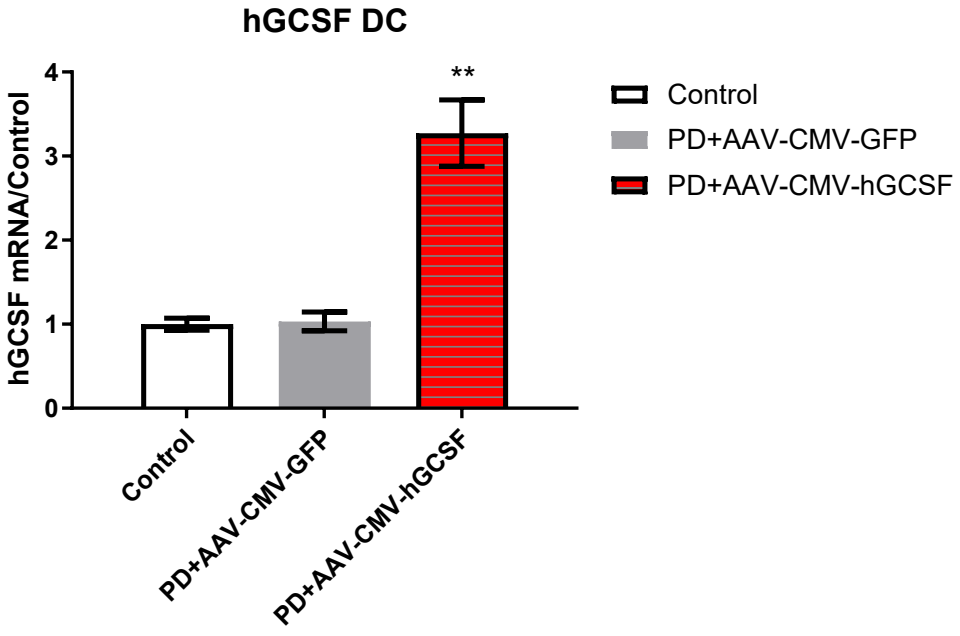

Figure 14. *qPCR quantification of hGCSF mRNA in the diencephalon of Parkinson's disease mice 7 days after delivery of AAV-CMV-hGCSF gene vector via eye drop. PD mice treated with AAV-CMV GCSF show >3-fold change in expression of hGCSF mRNA compared to PD mouse treated with AAV-CMV-GFP on day 7. (n=2 Error bars indicate the standard error of the mean)*

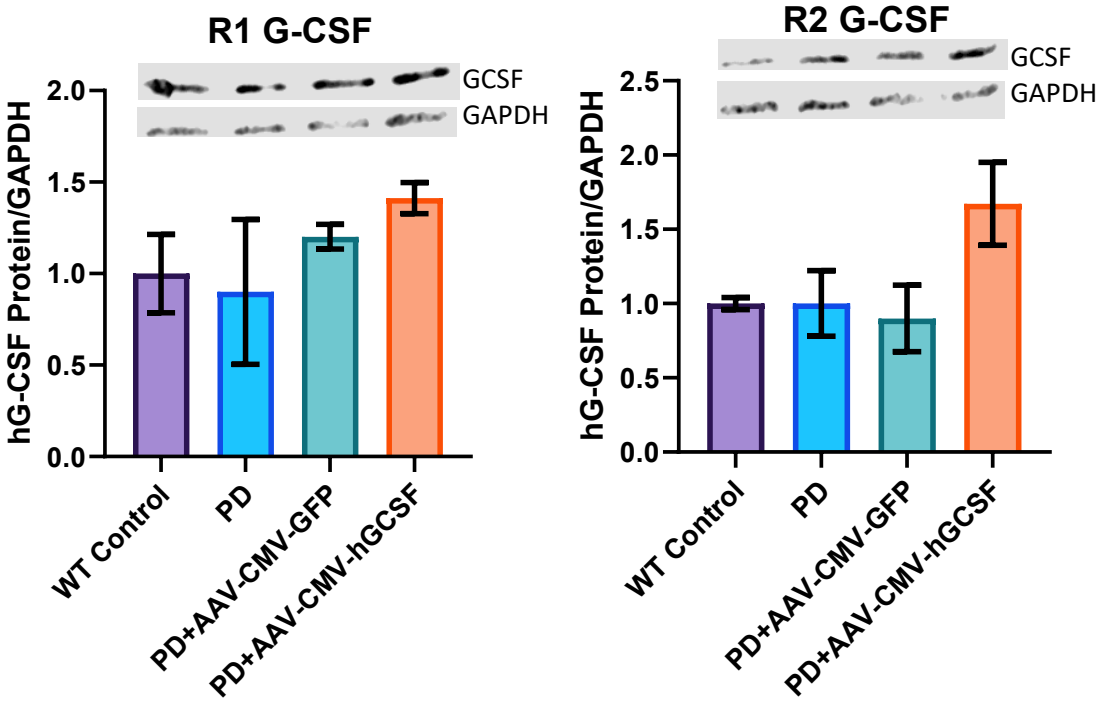

Figure 15. *Protein expression of hGCSF 7 days after gene therapy was delivered via eye drop. In the R1 forebrain region of the brain, a slight increase in GCSF was detected. In the R2 midbrain region, hGCSF expression was significantly increased in the gene therapy group. (n=2 Error bars indicate the standard error of the mean)*

3.3 Change in Tyrosine Hydroxylase following Gene Therapy

Then we measured both RNA and protein expression of tyrosine hydroxylase, a marker of dopamine neurons in mice 7 days after receiving AAV-CMV-hGCSF gene therapy. The wild type control and A53T mice that received AAV-CMV-GFP vector had no differences in GCSF expression in the basal ganglia (**Figure 16**) or diencephalon (**Figure 17**). Tyrosine hydroxylase mRNA expression increased 10-fold in the basal ganglia compared to the control. Tyrosine hydroxylase mRNA expression increased 13-fold in the diencephalon compared to the control. In the western blot for tyrosine hydroxylase, no differences were seen in the R1 region of the brain. However, in the R2 midbrain region, Parkinson's mice appeared to have a higher concentration of tyrosine hydroxylase compared to the control. AAV-CMV-hGCSF appeared to increase the level of tyrosine hydroxylase that was detected (**Figure 18**).

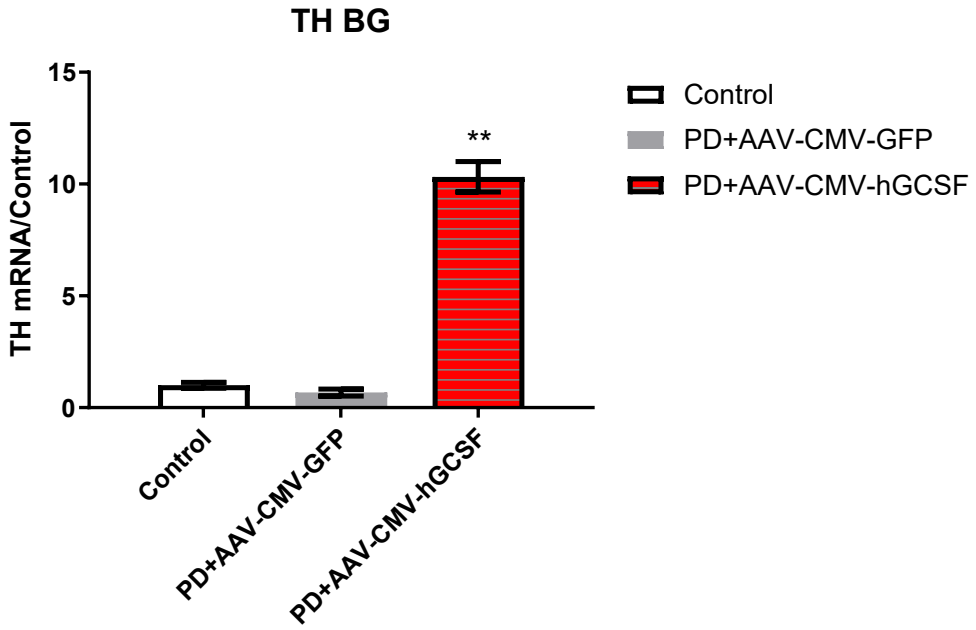

Figure 16. *qPCR quantification of tyrosine hydroxylase mRNA in the basal ganglia of Parkinson's disease mice 7 days after delivery of AAV-CMV-hGCSF gene vector via eye drop. PD mice treated with AAV-CMV-GCSF show >10-fold change in expression of tyrosine hydroxylase mRNA compared to PD mice. (n=2 Error bars indicate the standard error of the mean)*

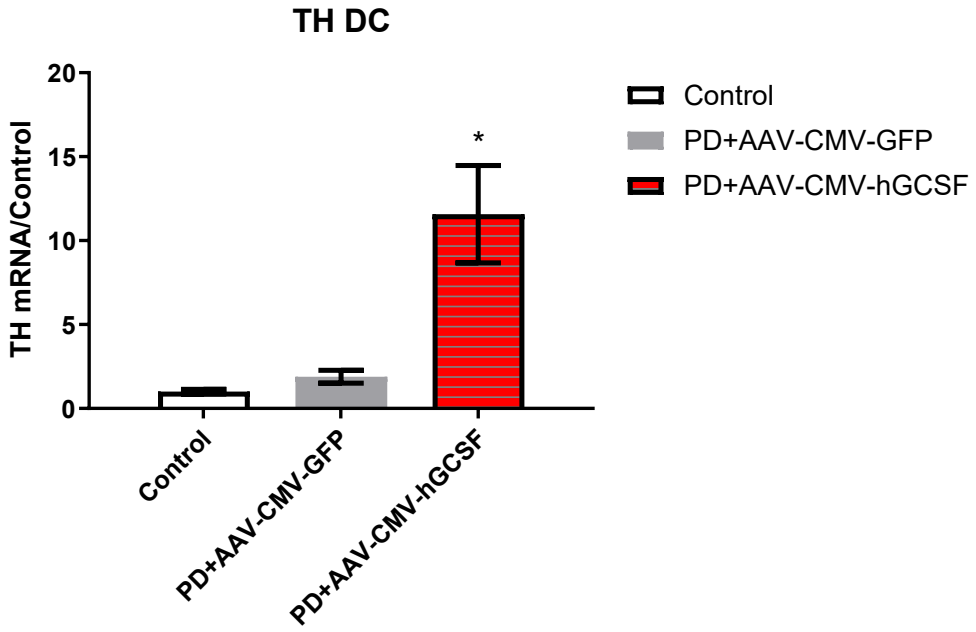

Figure 17. *qPCR quantification of tyrosine hydroxylase mRNA in the diencephalon of Parkinson's disease mice 7 days after delivery of AAV-CMV-hGCSF gene vector via eye drop. PD mice treated with AAV-CMV-GCSF show >12-fold change in expression of Tyrosine Hydroxylase mRNA. (n=2 Error bars indicate the standard error of the mean)*

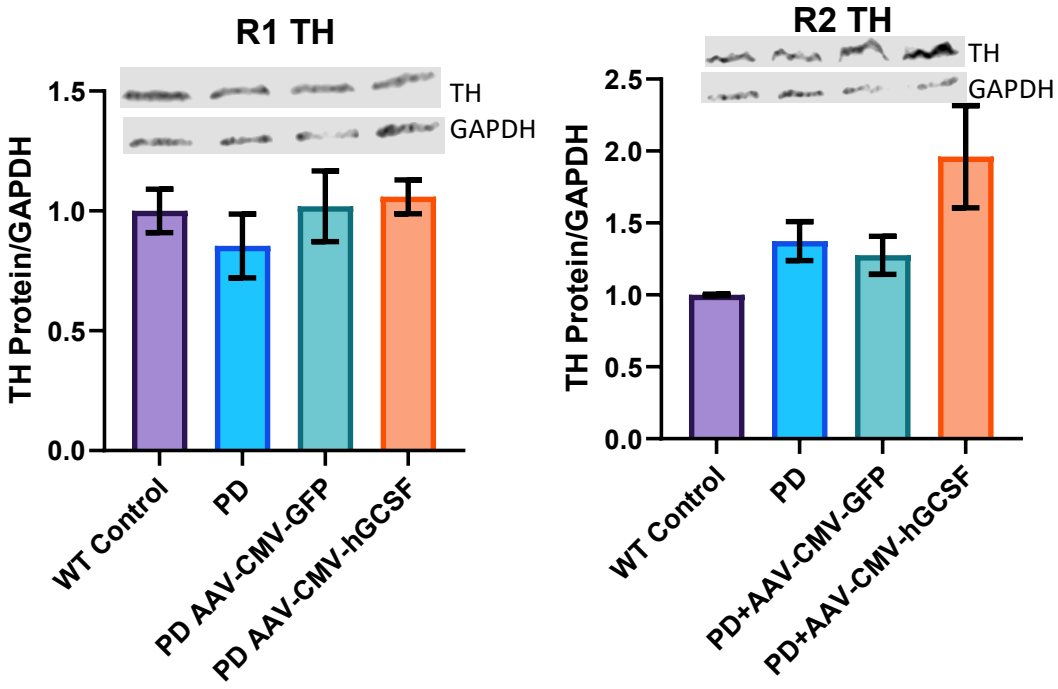

Figure 18. *Protein expression of tyrosine hydroxylase 7 days after gene therapy was delivered via eye drop. In the R1 forebrain region of the brain, no change in Tyrosine Hydroxylase was detected. In the R2 midbrain region, tyrosine hydroxylase expression was increased in the gene therapy group. Notability, tyrosine hydroxylase expression was higher in the Parkinson's mouse compared to the wild type control. (n=2 Error bars indicate the standard error of the mean)*

4.4 Change in KAT-2 following Gene Therapy

To see how a key step in the kynurenine pathway might change following GCSF gene therapy, we then did a western blot for KAT2. In the R1 forebrain region, the Parkinson's mice had reduced levels of KAT2. Wide variations in the standard error bars of vector and gene therapy groups makes it difficult to draw a conclusion in those groups. In the R2 midbrain region, a clearer difference emerged. The Parkinson's mice had elevated levels of KAT2 compared to the WT control. The PD+AAV-CMV-hGCSF group then restored KAT 2 back to the level of the WT control (**Figure 19**).

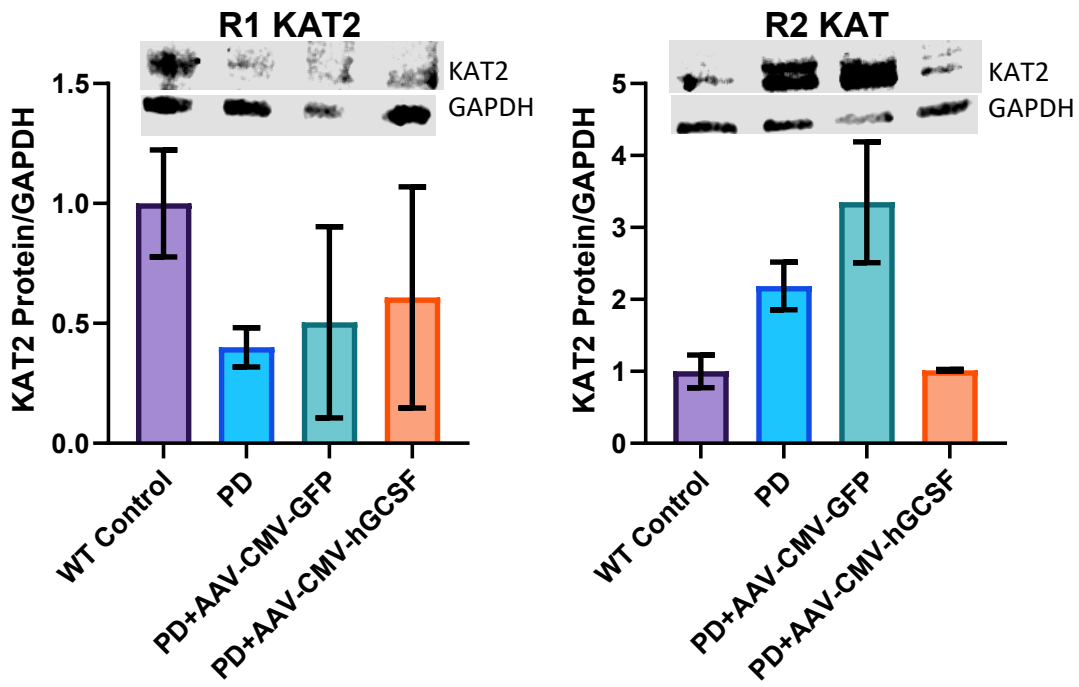

Figure 19 *Protein expression of KAT2 7 days after gene therapy was delivered via eye drop. In the R1 forebrain, PD mice appeared to have reduced expression of KAT2 compared to the WT control. A wide variation in the vector and hGCSF treatment groups makes it impossible to form a reliable hypothesis about KAT2 expression. In the R2 midbrain region, PD mice show higher expression of KAT2 compared to the WT control. hGCSF gene therapy restores the normal level of KAT-2. (n=2 Error bars indicate the standard error of the mean)*

CHAPTER 4: DISCUSSION

Here we offer a comprehensive look into the influence of various stimulants in triggering elements of the kynurenine pathway in astrocytes, microglia, and macrophage. Our protocol involved incubating cells for 24 hours with either IFNγ, IL-4, LPS, or saline and then measuring the levels of 5 different kynurenine pathway metabolites. In our trials with A172 astrocytes, we saw significant differences in a kynurenine metabolite in at least one of the conditions. In HMC3 microglia and Raw 264.7 macrophage the only statistically confirmed difference was in tryptophan.

Without a doubt, the strongest effect was seen in IFNγ which significantly depleted tryptophan in all three cell lines. Three enzymes are known to catabolize tryptophan into kynurenine, Indoleamine 2,3-dioxygenase 1 (IDO1), Indoleamine 2,3-dioxygenase 2(IDO2), and Tryptophan 2,3-dioxygenase (TDO).[82] Upregulation of IDO1 by IFNγ in a cell line was reported as early 1988.[83,84] IDO2 which has a highly similar sequence to IDO1 is also known to be upregulated by IFNγ.[85,86] Lastly TDO, whose significance in CNS kynurenine production is thought to be marginal may also be induced by IFNγ.[82] IFNγ has wide ranging effects downstream of the tryptophan degradation. In skin-derived fibroblasts treated with IFNγ, expression of the KATs were altered. KAT1 and KAT2 were increased, while KAT3 and KAT4 was either unchanged or reduced. The same study found that enzymes that lead to the production of quinolinic acid including Kynurenine 3-Monoxygenase, Hydroxyanthranilic acid oxygenase, and

Quinolinic Acid Phosphoribosyl Transferase were unchanged by IFNγ stimulation while Kynureninase is enhanced by IFNγ.[87]

IL-4 did not seem to affect tryptophan in any cell line and yet went on to result in increased kynurenine in A172 cells. Existing evidence suggests that IL-4 inhibits IDO expression in various cell lines and human monocytes[88] but enhances IDO expression when accompanied by IFNγ in microglia.[89] IL-4 stimulation of human keratinocytes does not affect either IDO or Kynureninase.[90]

LPS increased the amount of kynurenine in the media with A53T and HMC3 cells in our study, though the increase was only statistically significant in the former. This increase was in line with a previous study that found that LPS stimulation of a microglia cell line enhanced transcription of IDO and KMO. This same study also found that LPS increased kynurenine and quinolinic Acid present in the media.[91] In a mouse model, peripheral LPS administration resulted in increases in IDO1 but not IDO2 or TDO in the hippocampus, amygdala, and striatum.[92]

In the second part of our study, we evaluate the ability of hGCSF gene therapy to alter expression of granulocyte colony stimulating factor, tyrosine hydroxylase and kynurenine aminotransferase 2 in a mouse model of Parkinson's disease. The ability of AAV-CMV-hGCSF to express granulocyte colony stimulating factor in mice is well established. A previous study used an MRI based noninvasive tracking technique to validate delivery of the same gene therapy previously.[80] In our study, we used quantitative RT-PCR and western blotting to verify both transcription and translation of the therapeutic gene.

Tyrosine hydroxylase is an enzyme critical to dopamine production and neurons that contain it degenerate remarkably in patients with Parkinson's disease.[93] Our study found that gene therapy increased mRNA expression of tyrosine hydroxylase in the basal ganglia and diencephalon. Increased protein expression of tyrosine hydroxylase was observed in the midbrain, an area that typically sees remarkable tyrosine hydroxylase loss in the progression of Parkinson's disease. This report reiterates an earlier finding from our lab where GCSF protein restored tyrosine hydroxylase-positive neurons in the SNpc of MPTP Parkinson's mice. In-vivo microdialysis in that study showed that GCSF could restore striatal dopamine to levels equivalent to the MPTP free saline control.[59]

To our surprise, we found that Kynurenine Aminotransferase 2 is elevated in the midbrain of our mouse model of Parkinson's disease. We report that GCSF gene therapy was then able to restore the elevated level of KAT2 in Parkinson's mice to the level seen in WT mice. Interpretation of this data must be made with two major considerations. First, KAT2 is only one of 4 isoforms of kynurenine aminotransferase that is responsible for producing kynurenic acid.[94] The four mouse kynurenine aminotransferases were found to have varying biochemical properties such as varying levels of inhibition by methionine and optimal pH.[95] Secondly the contribution the four kynurenine aminotransferases to kynurenine production in mouse, rat, and human brain tissue may differ in ways that complicate interpretation. For example, while in humans and rats KAT2 mainly localizes to astrocytes, it was found to be localize to Perkinje cells and other neurons in mice.[93,96,97]

In our study, we investigated the wide-ranging effects of IFNγ, IL-4, and LPS on kynurenine pathway metabolites in microglia, macrophage, and astrocytes. We also

describe the neuroprotective effects of GCSF gene therapy in a mouse model of Parkinson's disease. We conclude that GCSF gene therapy may be therapeutic in Parkinson's disease by restoring kynurenine pathway dysfunction. Further research is needed to fully elucidate this possible mechanism.

REFERENCES

1. de Lau LM, Breteler MM. Epidemiology of Parkinson's disease. *Lancet Neurology*. 2006;5(6):525-535. doi:10.1016/S1474-4422(06)70471-9

2. Boggio PS, Ferrucci R, Rigonatti SP, et al. Effects of transcranial direct current stimulation on working memory in patients with Parkinson's disease. *Journal of the Neurological Sciences*. 2006;249(1):31-38. doi:10.1016/J.JNS.2006.05.062

3. Todorova A, Jenner P, Ray Chaudhuri K. Non-motor Parkinson's: integral to motor Parkinson's, yet often neglected. *Practical neurology*. 2014;14(5):310-322. doi:10.1136/practneurol-2013-000741

4. Chaudhuri KR, Healy DG, Schapira AH. Non-motor symptoms of Parkinson's disease: diagnosis and management. *The Lancet Neurology*. 2006;5(3):235-245. doi:10.1016/S1474-4422(06)70373-8

5. Sveinbjornsdottir S. The clinical symptoms of Parkinson's disease. *Journal of Neurochemistry*. 2016;139:318-324. doi:10.1111/jnc.13691

6. Dauer W, Przedborski S. Parkinson's disease: Mechanisms and models. *Neuron*. 2003;39(6):889-909. doi:10.1016/S0896-6273(03)00568-3

7. Dickson DW. Parkinson's disease and parkinsonism: Neuropathology. *Cold Spring Harbor Perspectives in Medicine*. 2012;2(8). doi:10.1101/cshperspect.a009258

8. Calne DB, Mizuno Y. The neuromythology of Parkinson's Disease. *Parkinsonism & Related Disorders*. 2004;10(5):319-322. doi:10.1016/J.PARKRELDIS.2004.03.006

9. Jellinger KA. A critical evaluation of current staging of α-synuclein pathology in Lewy body disorders. *Biochimica et Biophysica Acta (BBA) - Molecular Basis of Disease*. 2009;1792(7):730-740. doi:10.1016/J.BBADIS.2008.07.006

10. Briggs R, Kennelly SP, O'Neill D. Drug treatments in Alzheimer's disease. *Clinical medicine (London, England)*. 2016;16(3):247-253. doi:10.7861/clinmedicine.16-3-247

11. Knopman DS, Jones DT, Greicius MD. Failure to demonstrate efficacy of aducanumab: An analysis of the EMERGE and ENGAGE trials as reported by Biogen, December 2019. *Alzheimer's and Dementia*. 2021;17(4):696-701. doi:10.1002/alz.12213

12. Tolar M, Abushakra S, Hey JA, Porsteinsson A, Sabbagh M. Aducanumab, gantenerumab, BAN2401, and ALZ-801 - The first wave of amyloid-targeting drugs for Alzheimer's disease with potential for near term approval. *Alzheimer's Research and Therapy*. 2020;12(1):1-10. doi:10.1186/s13195-020-00663-w

13. Hornykiewicz O. A brief history of levodopa. In: *Journal of Neurology*. Vol 257. Springer; 2010:249-252. doi:10.1007/s00415-010-5741-y

14. Ellis JM, Fell MJ. Current approaches to the treatment of Parkinson's Disease. *Bioorganic and Medicinal Chemistry Letters*. 2017;27(18):4247-4255. doi:10.1016/j.bmcl.2017.07.075

15. Marek K, Jennings D, Seibyl J. Do dopamine agonists or levodopa modify Parkinson's disease progression? *European Journal of Neurology*. 2002;9(SUPPL. 3):15-22. doi:10.1046/j.1468-1331.9.s3.2.x

16. Raza C, Anjum R, Shakeel N ul A. Parkinson's disease: Mechanisms, translational models and management strategies. *Life Sciences*. 2019;226:77-90. doi:10.1016/j.lfs.2019.03.057

17. O. Watzlawik J, Wootla B, Rodriguez M. Tryptophan Catabolites and Their Impact on Multiple Sclerosis Progression. *Current Pharmaceutical Design*. Published online 2015. doi:10.2174/1381612822666151215095940

18. Ruddick JP, Evans AK, Nutt DJ, Lightman SL, Rook GAW, Lowry CA. Tryptophan metabolism in the central nervous system: Medical implications. *Expert Reviews in Molecular Medicine*. 2006;8(20):1-27. doi:10.1017/S1462399406000068

19. Maddison DC, Giorgini F. The kynurenine pathway and neurodegenerative disease. *Seminars in Cell & Developmental Biology*. 2015;40:134-141. doi:10.1016/j.semcdb.2015.03.002

20. Guidetti P, Hoffman GE, Melendez-Ferro M, Albuquerque EX, Schwarcz R. Astrocytic localization of kynurenine aminotransferase II in the rat brain visualized by immunocytochemistry. *Glia*. 2007;55(1):78-92. doi:10.1002/glia.20432

21. Han Q, Cai T, Tagle DA, Li J. Structure, expression, and function of kynurenine aminotransferases in human and rodent brains. *Cellular and molecular life sciences : CMLS*. 2010;67(3):353-368. doi:10.1007/s00018-009-0166-4

22. Wyckelsma VL, Lindkvist W, Venckunas T, et al. Kynurenine aminotransferase isoforms display fiber-type specific expression in young and old human skeletal muscle. *Experimental Gerontology*. 2020;134:110880. doi:10.1016/j.exger.2020.110880

23. Nematollahi A, Sun G, Jayawickrama GS, Church WB. Kynurenine aminotransferase isozyme inhibitors: A review. *International Journal of Molecular Sciences*. 2016;17(6):946. doi:10.3390/ijms17060946

24. Cooper AJL, Shurubor YI, Dorai T, et al. ω-Amidase: An underappreciated, but important enzyme in l-glutamine and l-asparagine metabolism; Relevance to sulfur and nitrogen metabolism, tumor biology and hyperammonemic diseases. *Amino Acids*. 2016;48(1):1-20. doi:10.1007/s00726-015-2061-7

25. Yoshida Y, Fujigaki H, Kato K, et al. Selective and competitive inhibition of kynurenine aminotransferase 2 by glycyrrhizic acid and its analogues. *Scientific Reports*. 2019;9(1):1-11. doi:10.1038/s41598-019-46666-y

26. Moroni F, Russi P, Carlá V, Lombardi G. Kynurenic acid is present in the rat brain and its content increases during development and aging processes. *Neuroscience Letters*. 1988;94(1-2):145-150. doi:10.1016/0304-3940(88)90285-6

27. Żarnowski T, Chorągiewicz T, Tulidowicz-Bielak M, et al. Ketogenic diet increases concentrations of kynurenic acid in discrete brain structures of young and adult rats. *Journal of neural transmission (Vienna, Austria : 1996)*. 2012;119(6):679-684. doi:10.1007/s00702-011-0750-2

28. Alkondon M, Pereira EFR, Yu P, et al. Targeted Deletion of the Kynurenine Aminotransferase II Gene Reveals a Critical Role of Endogenous Kynurenic Acid in the Regulation of Synaptic Transmission via 7 Nicotinic Receptors in the Hippocampus. Published online 2004. doi:10.1523/JNEUROSCI.5631-03.2004

29. Dobelis P, Varnell AL, Staley KJ, Cooper DC. Nicotinic α7 acetylcholine receptor-mediated currents are not modulated by the tryptophan metabolite kynurenic acid in adult hippocampal interneurons. *Nature*. 2011;(February 2015):20-21. doi:10.1038/npre.2011.6277.1

30. Albuquerque EX, Schwarcz R. Kynurenic acid as an antagonist of α7 nicotinic acetylcholine receptors in the brain: Facts and challenges. *Biochemical Pharmacology*. 2013;85(8):1027-1032. doi:10.1016/J.BCP.2012.12.014

31. Phani S, Loike JD, Przedborski S. Neurodegeneration and Inflammation in Parkinson's disease. *Parkinsonism & Related Disorders*. 2012;18:S207-S209. doi:10.1016/S1353-8020(11)70064-5

32. Devos D, Lebouvier T, Lardeux B, et al. Colonic inflammation in Parkinson's disease. *Neurobiology of Disease*. 2013;50:42-48. doi:10.1016/J.NBD.2012.09.007

33. Pierozan P, Biasibetti-Brendler H, Schmitz F, Ferreira F, Pessoa-Pureur R, Wyse ATS. Kynurenic Acid Prevents Cytoskeletal Disorganization Induced by Quinolinic Acid in Mixed Cultures of Rat Striatum. *Molecular Neurobiology*. 2018;55(6):5111-5124. doi:10.1007/s12035-017-0749-2

34. Wang J, Simonavicius N, Wu X, et al. Kynurenic acid as a ligand for orphan G protein-coupled receptor GPR35. *The Journal of biological chemistry*. 2006;281(31):22021-22028. doi:10.1074/jbc.M603503200

35. Tavassoly O, Sade D, Bera S, Shaham-Niv S, Vocadlo DJ, Gazit E. Quinolinic Acid Amyloid-like Fibrillar Assemblies Seed α-Synuclein Aggregation. Published online 2018. doi:10.1016/j.jmb.2018.08.002

36. Savitz J, Drevets WC, Smith CM, et al. Putative neuroprotective and neurotoxic kynurenine pathway metabolites are associated with hippocampal and amygdalar volumes in subjects with major depressive disorder. *Neuropsychopharmacology : official publication of the American College of Neuropsychopharmacology*. 2015;40(2):463-471. doi:10.1038/npp.2014.194

37. Lim J, Bang Y, Choi HJ. Abnormal hippocampal neurogenesis in Parkinson's disease: relevance to a new therapeutic target for depression with Parkinson's disease. *Archives of Pharmacal Research*. 2018;41(10):943-954. doi:10.1007/s12272-018-1063-x

38. Reijnders JSAM, Ehrt U, Weber WEJ, Aarsland D, Leentjens AFG. A systematic review of prevalence studies of depression in Parkinson's disease. *Movement Disorders*. 2008;23(2):183-189. doi:10.1002/mds.21803

39. Schuff N, Woerner N, Boreta L, et al. MRI of hippocampal volume loss in early Alzheimer's disease in relation to ApoE genotype and biomarkers. *Brain : a journal of neurology*. 2009;132(Pt 4):1067-1077. doi:10.1093/brain/awp007

40. Kokiko-Cochran ON, Godbout JP. The Inflammatory Continuum of Traumatic Brain Injury and Alzheimer's Disease. *Frontiers in Immunology*. 2018;9:672. doi:10.3389/fimmu.2018.00672

41. Oliva AA, Jiang M, Lam T, et al. Novel hippocampal interneuronal subtypes identified using transgenic mice that express green fluorescent protein in GABAergic interneurons. *The Journal of neuroscience : the official journal of the Society for Neuroscience*. 2000;20(9):3354-3368. doi:10.1523/jneurosci.5631-03.2004

42. Rodríguez-Arellano JJ, Parpura V, Zorec R, Verkhratsky A. Astrocytes in physiological aging and Alzheimer's disease. *Neuroscience*. 2016;323:170-182. doi:10.1016/J.NEUROSCIENCE.2015.01.007

43. Chun H, Lee CJ. Reactive astrocytes in Alzheimer's disease: A double-edged sword. *Neuroscience Research*. 2018;126:44-52. doi:10.1016/J.NEURES.2017.11.012

44. Meraz-Ríos MA, Toral-Rios D, Franco-Bocanegra D, Villeda-Hernández J, Campos-Peña V. Inflammatory process in Alzheimer's Disease. *Frontiers in integrative neuroscience*. 2013;7:59. doi:10.3389/fnint.2013.00059

45. Alasmari F, Alshammari MA, Alasmari AF, Alanazi WA, Alhazzani K. Neuroinflammatory Cytokines Induce Amyloid Beta Neurotoxicity through Modulating Amyloid Precursor Protein Levels/Metabolism. *BioMed Research International*. 2018;2018:1-8. doi:10.1155/2018/3087475

46. Hensley K, Carney JM, Mattson MP, et al. *A Model for Beta-Amyloid Aggregation and Neurotoxicity Based on Free Radical Generation by the Peptide: Relevance to Alzheimer Disease.* Vol 91.; 2006. doi:10.1073/pnas.91.8.3270

47. Grathwohl SA, Kälin RE, Bolmont T, et al. Formation and maintenance of Alzheimer's disease β-amyloid plaques in the absence of microglia. *Nature Neuroscience*. 2009;12(11):1361-1363. doi:10.1038/nn.2432

48. Villarán RF, Espinosa-Oliva AM, Sarmiento M, et al. Ulcerative colitis exacerbates lipopolysaccharide-induced damage to the nigral dopaminergic system: potential risk factor in Parkinson`s disease. *Journal of Neurochemistry*. 2010;114(6):1687-1700. doi:10.1111/j.1471-4159.2010.06879.x

49. Blum-Degena D, Müller T, Kuhn W, Gerlach M, Przuntek H, Riederer P. Interleukin-1β and interleukin-6 are elevated in the cerebrospinal fluid of Alzheimer's and de novo Parkinson's disease patients. *Neuroscience Letters*. 1995;202(1-2):17-20. doi:10.1016/0304-3940(95)12192-7

50. Chakrabarty P, Jansen-West K, Beccard A, et al. Massive gliosis induced by interleukin-6 suppresses Abeta deposition in vivo: evidence against inflammation as a driving force for amyloid deposition. *FASEB journal : official publication of the Federation of American Societies for Experimental Biology*. 2010;24(2):548-559. doi:10.1096/fj.09-141754

51. Aschner M. Immune and inflammatory responses in the CNS: modulation by astrocytes. *Toxicology Letters*. 1998;102-103:283-287. doi:10.1016/S0378-4274(98)00324-5

52. Testa U, Levi G, Peschle Aloisi CF, et al. *Production of Hemolymphopoietic Cytokines*.; 2019. Accessed July 3, 2019. http://www.jimmunol.org/content/149/7/2358

53. Hashioka S, Klegeris A, Schwab C, Yu S, McGeer PL. Differential expression of interferon-γ receptor on human glial cells in vivo and in vitro. *Journal of Neuroimmunology*. 2010;225(1-2):91-99. doi:10.1016/j.jneuroim.2010.04.023

54. Sanchez-Ramos J, Song S, Sava V, et al. GRANULOCYTE COLONY STIMULATING FACTOR DECREASES BRAIN AMYLOID BURDEN AND REVERSES COGNITIVE IMPAIRMENT IN ALZHEIMER'S MICE. *NSC*. 163:55-72. doi:10.1016/j.neuroscience.2009.05.071

55. Solaroglu I, Cahill J, Jadhav V, Zhang JH. A novel neuroprotectant granulocyte-colony stimulating factor. *Stroke*. 2006;37(4):1123-1128. doi:10.1161/01.STR.0000208205.26253.96

56. Modi J, Menzie-Suderam J, Xu H, et al. Mode of action of granulocyte-colony stimulating factor (G-CSF) as a novel therapy for stroke in a mouse model. *Journal of Biomedical Science*. 2020;27(1):19. doi:10.1186/s12929-019-0597-7

57. Dumbuya JS, Chen L, Shu SY, et al. G-CSF attenuates neuroinflammation and neuronal apoptosis via the mTOR/p70SK6 signaling pathway in neonatal Hypoxia-Ischemia rat model. *Brain Research*. 2020;1739:146817. doi:10.1016/j.brainres.2020.146817

58. Ding J, Yu J-Z, Li Q-Y, Wang X, Lu C-Z, Xiao B-G. Rho kinase inhibitor Fasudil induces neuroprotection and neurogenesis partially through astrocyte-derived G-

CSF. *Brain, Behavior, and Immunity*. 2009;23(8):1083-1088. doi:10.1016/J.BBI.2009.05.002

59. McCollum M, Ma Z, Cohen E, et al. Post-MPTP Treatment with Granulocyte Colony-Stimulating Factor Improves Nigrostriatal Function in the Mouse Model of Parkinson's Disease. *Molecular Neurobiology*. 2010;41(2-3):410-419. doi:10.1007/s12035-010-8118-4

60. Jiang H, Liu CX, Feng JB, et al. *Granulocyte Colony-Stimulating Factor Attenuates Chronic Neuroinflammation in the Brain of Amyloid Precursor Protein Transgenic Mice: An Alzheimer's Disease Mouse Model*.; 2010. Accessed January 16, 2019. https://journals.sagepub.com/doi/pdf/10.1177/147323001003800412

61. Schneider A, Krüger C, Steigleder T, et al. The hematopoietic factor G-CSF is a neuronal ligand that counteracts programmed cell death and drives neurogenesis. *The Journal of clinical investigation*. 2005;115(8):2083-2098. doi:10.1172/JCI23559

62. Bendall LJ, Bradstock KF. G-CSF: From granulopoietic stimulant to bone marrow stem cell mobilizing agent. *Cytokine & Growth Factor Reviews*. 2014;25(4):355-367. doi:10.1016/J.CYTOGFR.2014.07.011

63. Capes-Davis A, Theodosopoulos G, Atkin I, et al. Check your cultures! A list of cross-contaminated or misidentified cell lines. *International Journal of Cancer*. 2010;127(1):1-8. doi:10.1002/ijc.25242

64. Nikfarjam L, Farzaneh P. Prevention and Detection of Mycoplasma Contamination in Cell Culture. *Cell Journal (Yakhteh)*. 2012;13(4):203. Accessed April 19, 2019. https://www.ncbi.nlm.nih.gov/pmc/articles/PMC3584481/

65. Çelik-Uzuner S, Uzuner U. An Extensive Method for Maintenance of Sterility in Mammalian Cell Culture Laboratory Routine. *Challenges*. 2017;8(2):26. doi:10.3390/challe8020026

66. Meredith GE, Rademacher DJ. MPTP mouse models of Parkinson's disease: An update. *Journal of Parkinson's Disease*. 2011;1(1):19-33. doi:10.3233/JPD-2011-11023

67. William Langston J, Forno LS, Rebert CS, Irwin I. Selective nigral toxicity after systemic administration of 1-methyl-4-phenyl-1,2,5,6-tetrahydropyrine (MPTP) in the squirrel monkey. *Brain Research*. 1984;292(2):390-394. doi:10.1016/0006-8993(84)90777-7

68. Sonsalla PK, Heikkila RE. The influence of dose and dosing interval on MPTP-induced dopaminergic neurotoxicity in mice. *European Journal of Pharmacology*. 1986;129(3):339-345. doi:10.1016/0014-2999(86)90444-9

69. Ricaurte GA, William Langston J, Delanney LE, Irwin I, Peroutka SJ, Forno LS. Fate of nigrostriatal neurons in young mature mice given 1-methyl-4-phenyl-1,2,3,6-tetrahydropyridine: A neurochemical and morphological reassessment. *Brain Research*. 1986;376(1):117-124. doi:10.1016/0006-8993(86)90905-4

70. Chadi G, Mø11er A, Rosen L, et al. Protective actions of human recombinant basic fibroblast growth factor on MPTP-lesioned nigrostriatal dopamine neurons after

intraventricular infusion. *Experimental Brain Research*. 1993;97(1):145-158. doi:10.1007/BF00228825

71. Jagmag SA, Tripathi N, Shukla SD, Maiti S, Khurana S. Evaluation of models of Parkinson's disease. *Frontiers in Neuroscience*. 2016;9(JAN):503. doi:10.3389/fnins.2015.00503

72. Dauer W, Kholodilov N, Vila M, et al. Resistance of α-synuclein null mice to the parkinsonian neurotoxin MPTP. *Proceedings of the National Academy of Sciences of the United States of America*. 2002;99(22):14524-14529. doi:10.1073/pnas.172514599

73. Masliah E, Rockenstein E, Veinbergs I, et al. Dopaminergic loss and inclusion body formation in α-synuclein mice: Implications for neurodegenerative disorders. *Science*. 2000;287(5456):1265-1269. doi:10.1126/science.287.5456.1265

74. Nuber S, Petrasch-Parwez E, Winner B, et al. Neurodegeneration and motor dysfunction in a conditional model of Parkinson's disease. *Journal of Neuroscience*. 2008;28(10):2471-2484. doi:10.1523/JNEUROSCI.3040-07.2008

75. Fernagut PO, Chesselet MF. Alpha-synuclein and transgenic mouse models. *Neurobiology of Disease*. 2004;17(2):123-130. doi:10.1016/j.nbd.2004.07.001

76. Giasson BI, Duda JE, Quinn SM, Zhang B, Trojanowski JQ, Lee VMY. Neuronal α-synucleinopathy with severe movement disorder in mice expressing A53T human α-synuclein. *Neuron*. 2002;34(4):521-533. doi:10.1016/S0896-6273(02)00682-7

77. Graham DR, Sidhu A. Mice expressing the A53T mutant form of human alpha-synuclein exhibit hyperactivity and reduced anxiety-like behavior. *Journal of Neuroscience Research*. 2010;88(8):NA-NA. doi:10.1002/jnr.22331

78. Oaks AW, Frankfurt M, Finkelstein DI, Sidhu A. Age-Dependent Effects of A53T Alpha-Synuclein on Behavior and Dopaminergic Function. *PLoS ONE*. 2013;8(4):60378. doi:10.1371/journal.pone.0060378

79. Farrell KF, Krishnamachari S, Villanueva E, et al. Non-motor parkinsonian pathology in aging A53T α-Synuclein mice is associated with progressive synucleinopathy and altered enzymatic function. *Journal of Neurochemistry*. 2014;128(4):536-546. doi:10.1111/jnc.12481

80. Ren J, Chen YI, Liu CH, et al. Noninvasive tracking of gene transcript and neuroprotection after gene therapy. *Gene Therapy*. 2016;23(1):1-9. doi:10.1038/gt.2015.81

81. Allen Institute for Brain Science. Allen Brain Atlas: Mouse Brain. Published 2011. Accessed July 8, 2021. https://mouse.brain-map.org/static/atlas

82. Fujigaki H, Yamamoto Y, Saito K. L-Tryptophan-kynurenine pathway enzymes are therapeutic target for neuropsychiatric diseases: Focus on cell type differences. *Neuropharmacology*. 2017;112:264-274. doi:10.1016/j.neuropharm.2016.01.011

83. Takikawa O, Kuroiwa T, Yamazaki F, Kido R. Mechanism of interferon-γ action. Characterization of indoleamine 2,3-dioxygenase in cultured human cells induced by interferon -γ and evaluation of the enzyme-mediated tryptophan degradation in

its anticellular activity. *Journal of Biological Chemistry*. 1988;263(4):2041-2048. doi:10.1016/s0021-9258(19)77982-4

84. Fujigaki S, Saito K, Takemura M, et al. L-tryptophan-L-kynurenine pathway metabolism accelerated by Toxoplasma gondii infection is abolished in gamma interferon-gene-deficient mice: Cross-regulation between inducible nitric oxide synthase and indoleamine-2,3-dioxygenase. *Infection and Immunity*. 2002;70(2):779-786. doi:10.1128/IAI.70.2.779-786.2002

85. Witkiewicz AK, Costantino CL, Metz R, et al. Genotyping and Expression Analysis of IDO2 in Human Pancreatic Cancer: A Novel, Active Target. *Journal of the American College of Surgeons*. 2009;208(5):781-787. doi:10.1016/j.jamcollsurg.2008.12.018

86. Löb S, Königsrainer A, Zieker D, et al. IDO1 and IDO2 are expressed in human tumors: Levo- but not dextro-1-methyl tryptophan inhibits tryptophan catabolism. *Cancer Immunology, Immunotherapy*. 2009;58(1):153-157. doi:10.1007/s00262-008-0513-6

87. Asp L, Johansson AS, Mann A, et al. Effects of pro-inflammatory cytokines on expression of kynurenine pathway enzymes in human dermal fibroblasts. *Journal of Inflammation*. 2011;8(1):1-7. doi:10.1186/1476-9255-8-25

88. Musso T, Gusella GL, Brooks A, Longo DL, Varesio L. Interleukin-4 inhibits indoleamine 2,3-dioxygenase expression in human monocytes. *Blood*. 1994;83(5):1408-1411. doi:10.1182/blood.v83.5.1408.1408

89. Yadav MC, Burudi EME, Alirezaei M, et al. IFN-γ-induced IDO and WRS expression in microglia is differentially regulated by IL-4. *GLIA*. 2007;55(13):1385-1396. doi:10.1002/glia.20544

90. Ito M, Ogawa K, Takeuchi K, et al. Gene expression of enzymes for tryptophan degradation pathway is upregulated in the skin lesions of patients with atopic dermatitis or psoriasis. *Journal of Dermatological Science*. 2004;36(3):157-164. doi:10.1016/j.jdermsci.2004.08.012

91. Garrison AM, Parrott JM, Tuñon A, Delgado J, Redus L, O'Connor JC. Kynurenine pathway metabolic balance influences microglia activity: Targeting kynurenine monooxygenase to dampen neuroinflammation. *Psychoneuroendocrinology*. 2018;94:1-10. doi:10.1016/j.psyneuen.2018.04.019

92. Parrott JM, Redus L, O'Connor JC. Kynurenine metabolic balance is disrupted in the hippocampus following peripheral lipopolysaccharide challenge. *Journal of Neuroinflammation*. 2016;13(1):1-15. doi:10.1186/s12974-016-0590-y

93. Nagatsu T, Nakashima A, Ichinose H, Kobayashi K. Human tyrosine hydroxylase in Parkinson's disease and in related disorders. *Journal of Neural Transmission*. 2019;126(4):397-409. doi:10.1007/s00702-018-1903-3

94. Han Q, Cai T, Tagle DA, Li J. Structure, expression, and function of kynurenine aminotransferases in human and rodent brains. *Cellular and Molecular Life Sciences 2009 67:3*. 2009;67(3):353-368. doi:10.1007/S00018-009-0166-4

95. Han Q, Cai T, Tagle DA, Li J. Thermal stability, pH dependence and inhibition of four murine kynurenine aminotransferases. *BMC Biochemistry 2010 11:1*. 2010;11(1):1-10. doi:10.1186/1471-2091-11-19

96. Balog E, Jenei G, Gellért L, et al. Species-specific neuronal localization of kynurenine aminotransferase-2 in the mouse cerebellum. *Neurochemistry International*. 2021;142:104920. doi:10.1016/J.NEUINT.2020.104920

97. Guidetti P, Hoffman GE, Melendez-Ferro M, Albuquerque EX, Schwarcz R. Astrocytic localization of kynurenine aminotransferase II in the rat brain visualized by immunocytochemistry. *Glia*. 2007;55(1):78-92. doi:10.1002/GLIA.20432